MAPPING SOIL VARIABILITY WITH A DECISION TREE MODELLING APPROACH IN THE NORTHERN HIGHLANDS OF ETHIOPIA

Hof, Susanne

In contrast to many other soil mapping surveys, which use a 'pure' conventional or digital soil mapping strategy, this is a study in which a more qualitative approach to digital soil mapping is used. The objective is to evaluate the use of decision tree models in order to map soil variability at a detailed resolution in poorly accessible landscapes using limited observations and available auxiliary information. A study area in the Northern Highlands of Ethiopia, is used to implement the conceptual method. The locally developed decision tree model is extrapolated to predict soil type for other representative areas in the region. The results of this study show that the spatial heterogeneity and complexity of the landscape in Northern Ethiopia can be sufficiently mapped with use of decision tree modelling. However, the limited amount of samples and auxiliary information clearly constrained the prediction accuracy.

MSC THESIS REPORT

MAPPING SOIL VARIABILITY WITH A DECISION TREE MODELLING APPROACH IN THE NORTHERN HIGHLANDS OF ETHIOPIA

MSC THESIS REPORT

SUSANNE HOF

SUPERVISORS: JETSE STOORVOGEL & RICHARD KRAAIJVANGER

MAY 2014

WAGENINGEN UNIVERSITY

TABLE OF CONTENTS

1 INTRODUCTION

Many land-use strategies are being adopted based on only one or few 'typical' situation(s) per country. To enable better land-use strategies and improve the livelihood of the population, knowledge of the spatial patterns of soil variation is required on a much more detailed scale. Traditionally this required a large amount of field observations (the common rule is 1-2 field observations per cm on the printed map; making nr. of observations dependent on the scale of the map). Of course, these intensive soil-surveys take a lot of time and effort, which make them very expensive.

The above mentioned method is a more conventional method in the sense that currently digital soil mapping (DSM) methods are used increasingly, due to some significant advantages. Conceptually, DSM and conventional soil mapping (CSM) are very similar. Both approaches use a soil-landscape model to predict soil properties at unobserved locations. The main difference is that in the case of CSM a qualitative model is derived based on expert knowledge of the surveyor and in DSM a quantitative model (in most cases a statistical model) is made based on auxiliary information from remote sensors and other data sources. The result from CSM is a general-purpose map with soil bodies being represented as discrete, homogeneous and simplified entities (with abrupt boundaries), while DSM typically results in specific-purpose maps where soil properties can be represented continuously in space. These specific purpose maps, relative to the general kind, can provide the soil information on the level of detail that is needed for many regional land-use analysis models, which could enable better land-use strategies. Furthermore, the advantages in DSM over CSM are that it is more efficient and cost effective in most cases, because it can be successful with a limited number of field observations (Cambule, Rossiter and Stoorvogel 2012, Kempen et al. 2012, Stoorvogel et al. 2009, Mora-Vallejo et al. 2008).

Although the technique is relatively new, literature already provides an increasing amount of examples where DSM is presented as an effective and efficient surveying technique. However in many of these cases the techniques are applied in small areas (less than 100 ha) with at least 200 observations per square kilometre, or for semi-detailed soil surveys in areas of less than 150 km2, in which the number of observations per square kilometre ranges from one to 20 (Mora-Vallejo et al. 2008). For the purpose of better land-use strategies we would require detailed soil variability information for the scope of the whole administrative region, which is more in the range of 20 000 km^2.

The success of DSM will mainly depend on the availability of up-to-date and high scaled soil data and environmental data layers, such as digital elevation models (DEM's), and satellite imagery representing land-cover, climate and other soil forming factors (Cambule et al. 2012, Kempen et al. 2012, Stoorvogel et al. 2009). Another issue in many underdeveloped countries, is the fact that DSM techniques are still difficult to implement due to the limited availability of quantitative information to support rigorous statistical models. In such a situation, instead of fitting a model to the data, decision tree models can be used. This is a method of data analysis whereby a rule-structure (in the form of a tree) is generated from qualitative information that is available from for example other studies (Stoorvogel et al. 2009, Taghizadeh-Mehrjardi et al. 2014). The qualitative information available in terms of soil catenas, general soil surveys, and soil classification studies can already give an insight in

the spatial patterns of the soil variability. Decision trees are easy to interpret and can handle both continuous and categorical data (Taghizadeh-Mehrjardi et al. 2014).

In this research, a limited amount of available auxiliary data will be used together with available qualitative information, in the form of soil catenas and classification studies to create decision tree models in order to map the soil variability of agricultural land in the Northern Highlands of Ethiopia. The following research question will be answered:

Can decision tree models successfully map soil variability at a high resolution in poorly accessible landscapes using limited observations and available auxiliary information?

The soil variability will be characterized by soil type and soil fertility properties. In turn, soil texture and organic matter content will be the mapped soil properties representing soil fertility. As a stable natural property, soil texture determines soil fertility to a great extent as it affects soil nutrient behaviours and water availability. Detailed soil spatial texture information is also required by land management applications (Wang et al. 2012). Soil organic matter (SOM) increases soil fertility by providing cation exchange sites and acting as reserve of essential (micro-)nutrients, especially nitrogen (N), which are slowly released upon SOM mineralization.

Before the creation of the model, a literature study, a quick aerial photograph interpretation and a small soil survey in the form of transects will be carried out in order to understand the general relationships of the spatial variability in soil types and properties. The focus will lay on only a small, but representative section of the total study area. The development of the models will be based on the availability of auxiliary data layers and the qualitative relationships found previously. The model will be validated in the small area with use of another independent dataset derived with a stratified-random sampling scheme, and tested for applicability (extrapolated) in at least one other area in the Central Tigray Highlands using random points. In total only 50 sample locations will be visited, because of time, money and logistical limitations.

This research is done in order to test the hypothesis that a hybrid method of conventional and digital soil mapping with use of decision tree models, can be effective ánd cost efficient on a large scale and with a regional scope, in poorly accessible and underdeveloped countries. The coefficient of determination or correlation coefficient (R^2) provides a measure of how well observed outcomes are replicated by the model, as the proportion of total variation of outcomes explained by the model. With the traditional soil type map, an accuracy of 50% is common, so this will be the threshold to call the resulting maps a success.

2 CONCEPTUAL METHOD

The conceptual method arose from the need to assess the soil variability in the Northern Highlands of Ethiopia (the study area will be introduced in Section 3.1.1) in order to improve the livelihood of the population who strongly depend on agriculture.

Like many other underdeveloped countries, existing knowledge of soil properties and its spatial distribution in Ethiopia are mostly limited to maps with a small scale (representing less detailed information for a large area, e.g. the soil map (BoANR-LUPRD 2000) and geological maps (Merla 1973, Mohr 1663) of Ethiopia) or with a small scope (more detail, but for a limited area e.g. Nyssen et al. (2008), Rabia et al. (2013) and Tesfamichael (2010)). To support sustainable land management, it is desired to have knowledge of soil properties on a larger scale and in the scope of the whole administrative region. However, detailed soil surveys for a large region are too expensive (especially for an underdeveloped country). In addition most of these areas are hard to access due to logistical limitations, such as bad roads or no roads, topographical obstructions and in some cases even dangers due to wildlife.

The digital soil mapping technique is very promising, because it has shown to be successful with the use of limited soil observations, reducing the survey cost significantly. The conceptual framework of digital soil mapping (DSM) is based on the original mechanistic model for soil development derived by Jenny (1941).

$$S = f(c,o,r,p,t).$$

This equation describes soil development in terms of five main soil forming factors, namely: climate (c), organisms (o, ranging from microorganisms to vegetation, but also including humans), relief (r), parent material (p) and time (t) (Stoorvogel et al. 2009, McBratney, Santos and Minasny 2003).

McBratney et al. (2003) describe in their review numerous ways to make digital soil maps based on geographic information systems (GIS) data layers, which will represent the above mentioned soil forming factors in relation to space. They propose the following conceptual model to predict soil attributes (S_a) and soil property classes (S_c):

$$S_{a/c} = f(\text{available auxiliary information}) = f(s,c,o,r,p,a,n)$$

Those seven factors stand for: soil properties at the same location (s), climate (c), organisms (o), relief (r), parent material (p), age (a) and geographic position (n). One could combine this auxiliary information with a limited number of field observations to derive the relationships between soil properties or classes and their position in the landscape. The landscape or terrain attributes are usually derived from digital elevation models (DEMs), representing topography, spectral reflectance bands from satellite images, representing land-cover and climate and (digital) geological maps, representing parent material and age. The implementation of this conceptual model is typically the derivation of a statistical relationship between the various explanatory variables and soil properties. Statistical models are in many cases able to explain a significant percentage of the spatial variation in the soil properties, although usually a significant amount of residual variation remains. If it has a spatial dependency, this remaining variation or residuals can be interpolated and described using regression-kriging (Hengl, Heuvelink and Stein 2004).

As mentioned before, the success of DSM will mainly depend on the availability of up-to-date and high scaled soil data and environmental data layers. Due to availability problems, we see that the soil variation is commonly induced by a limited number of soil forming factors. Although this seems incorrect, most attempts are effective using topography and some terrain attribute only. This is possible when the soil variability is largely due to the effect of topography on soil genesis (Mora-Vallejo et al. 2008, Cambule et al. 2012). This leads us to the conceptual model that is most used:

$S_{a/c}$ = f(available auxiliary information) + residuals.

The availability of quantitative information to sustain the statistical models, is also limited in the case of this research. Van de Wauw et al. (2008) already addressed this issue in their paper by stating that the landscape in question is too complex, while detailed georeferenced information is lacking for the desired mapping scale. Therefor they chose a more conventional method with use of aerial photograph interpretation. Despite the limited availability of quantitative data concerning all of the soil forming factors, there is some qualitative research done in the area (e.g. Nyssen et al. (2008); Rabia et al. (2013); Van de Wauw et al. (2008)). Before dismissing the digital approach right away, this qualitative information can open possibilities for more qualitative approaches to digital soil mapping (Stoorvogel et al. 2009), in a way that we can have the best of both approaches.

In situations like these we can develop decision tree models, instead of statistical models. This is a method of data analysis whereby a rule-structure (in the form of a tree) is generated from available qualitative information. In addition to an extensive literature review, one could relate (check) the found relationships by collecting additional observations. Based on the relationships found, the data are grouped, each division being chosen as to maximize some measure of difference in the target variable in the resulting groups (Stoorvogel et al. 2009, McBratney et al. 2003).

To acquire information about the soil variability on a regional scale there are two options: 1) small scale sampling and interpolation for the regional scope (e.g. Mora-Vallejo et al. (2008)), 2) large scale sampling in small local area and extrapolation to the larger/regional area. Concerning the desired detail, the second option would be preferred. Cambule et al. (2012) found that in cases of poor accessibility, one could model the relationships between soil forming explanatory variables and soil properties/types (target variables) in the accessible part and apply it in the inaccessible parts, under the condition that the inaccessible area(s) are similar to the accessible area. I reasoned that such an approach could be applicable in the Ethiopian Highlands, under the same condition. This way one could concentrate the observations in a small representative local area and extrapolate the findings to the surrounding region.

In summary, to preform predictive mapping of an regional area with poor accessibility, limited quantitative data availability and highly preferred cost efficiency, I propose to use a method based on DSM, but with use of a decision tree approach. The focus of the model development will be on a small and local area. The resulting model will be extrapolated to the rest of the representative landscape. The schematic of the conceptual method can be found in Figure 1.

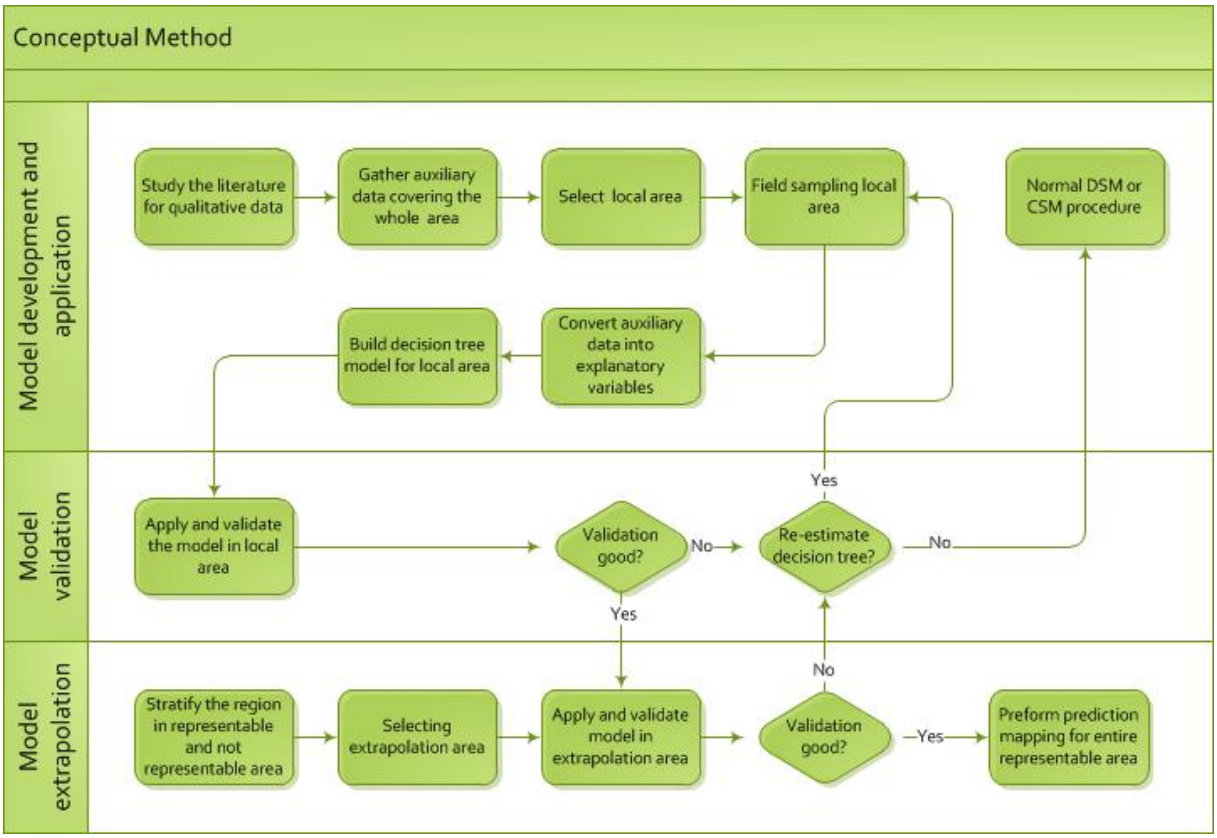

Figure 1: The general approach of the conceptual method.

The conceptual method involves three main steps: 1) the decision tree model development based on a literature study, transect soil survey in a small and accessible but representative area and available auxiliary information; 2) the model application and validation by assessing the models accuracy and explained variability with use of an independent 'validation dataset'; 3) the model extrapolation to the regional scope, by first checking the representation of the outer area and after the model is applied assessing its accuracy with use of another independent 'extrapolation dataset'.

The details to the implementation of this conceptual method will be discussed in the following chapter of materials and methods (Chapter 3). The results of the application will be discussed in Chapter 4.

3 MATERIALS AND METHODS

This chapter includes a description of the study area and the materials and methods behind the model development and application (Section 3.1), validation (Section 3.2) and extrapolation (Section 3.3).

3.1 MODEL DEVELOPMENT AND APPLICATION

The conceptual method requires three types of information that will be used as input for the decision tree model for the spatial prediction of soil type, texture and organic matter content. These are the qualitative information from the literature study (Section 3.1.1), additional acquired data (Section 3.1.2) and the available auxiliary data that needs to be categorized in explanatory variables (Section 3.1.3).

3.1.1 LITERATURE STUDY

Within this section, the study area will be introduced (Section 3.1.1.1). It will give an overview of the literature including the present knowledge on the topics of climate (Section 3.1.1.2), geology (Section 3.1.1.3), geomorphology (Section 3.1.1.4), land-use and land-cover (Section 3.1.1.5) and soil development (Section 3.1.1.6) in the Northern Highlands of Ethiopia. This knowledge will be used to determine the relationships explaining soil variability.

3.1.1.1 LOCATION

The study area lies in the far most Northern regional state of Ethiopia; the Tigray region in the Northern Highlands. Agriculture is the most important source of subsistence for the majority of the population. Tigray is one of Ethiopia's most food insecure regions. For example, an estimated 40% of the rural population in the central part of Tigray depends on food-aid, due to poor food security (Kraaijvanger et al. 2013). It is therefore essential to attain a better understanding of the soil variability and development in relation to soil forming factors, in order to enable better land-use strategies.

Within the centre of this region, four *woredas* (third level local administrative districts) are chosen, respectively; Werie-Leke, Hawzen, Ahforom and Dogua Tembien (Figure 2). The study area covers an area of approximately 10000 km^2 and has the typical elevation and geomorphology of the area that represents the whole of the Northern Ethiopian Highlands. The altitude in the study area varies from 1900 m up to 2600 m a.s.l.

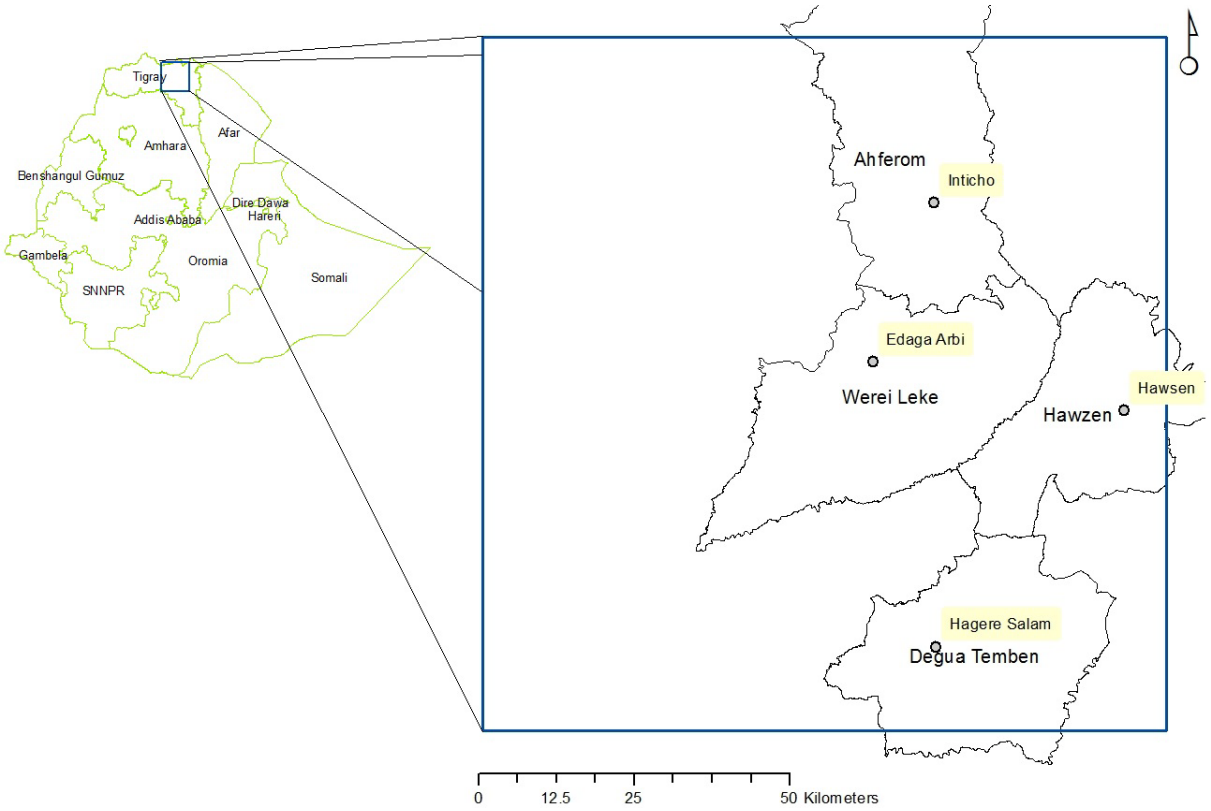

Figure 2: Location of the four woredas in Central- and East-Tigray, Ethiopia, with their administrative centres.

In accordance with Kraaijvanger et al. (2013), the names or abbreviations of their respective administrative centres will be used to indicate the four areas; Edaga Arbi (EA), Hawzen (HW), Inticho (IN) and Hagere Selam (HS). Near to the first town (EA) lays a typical land-unit; a table-mountain. This land-unit and its direct surrounding area, consisting of two river basins, will be used as the main study area with the purpose to make the model (Section 3.1.2 and 3.1.3). Small sections of the other three areas will be used in extrapolation of the model (Section 3.3).

3.1.1.2 CLIMATE

The central and eastern parts of Ethiopia, including our study area, have a tropical semi-arid climate with three distinctive seasons of which two rainy periods and one dry period. These seasons are locally known as the small *Belg* rains (February-May), main *Kiremt* rains (June –September), and dry *Bega* season (October-January) (USDA 2013). These weather cycles are the direct result of the location of the Intertropical Convergence Zone (ITCZ). The first season is characterised by short 'unreliable' rains, caused by the movement of the ITCZ from South of the equator to the North (Nyssen et al. 2005). The second season is identified by long and heavy rains with violent thunderstorms, which is explained by the position of the ITCZ, being at its most northerly position during summer on the northern hemisphere. Generally, clouds are formed at the end of the morning, as a result of evaporation and convective cloud formation due to daytime heating of the land. This moisture will be released in the afternoon, when it cools. At the end of the summer, the ITCZ returns quickly to the South, preventing the production of rain showers (Nyssen et al. 2005). This marks the beginning of the dry season. During this last season, most of the highland in Ethiopia is sunny during

the day and cold during the night and morning, which includes frost at high altitudes in December and January (USDA 2013).

The amount of rain varies not only through the seasons, but is strongly related with altitude, relief and aspect, and is therefore also locally variable within the study areas. This can be explained by the convective nature of the main rain season. Slopes exposed to the west and north receive less sunshine (Nyssen et al. 2005). Annual precipitation ranges from 522 mm for HW to 683 mm for HS, and is highly erratic through the years (Kraaijvanger et al. 2013), because the location of the ITCZ can develop differently each year. Also temperature varies with altitude; according to Araya, Keesstra and Stroosnijder (2010) the average temperature ranges between 15 °C and 21.5 °C for altitudes ranging between 2000 and 2500 m a.s.l.

3.1.1.3 GEOLOGY

The regional geology of Tigray and the wider Ethiopian region plus Eritrea has been explored in cycles, some of the classic work being that of Blanford (1870); made during a British expedition, Dainelli and Marinelli (1912), Merla and Minucci (1938), Dainelli (1943); which are all Italians, Mohr (1962); for the University of Addis Abeba and Garland (1978, 1980); who wrote a 51 paged book about the geology in the Adigrat area, which lays directly east from the study area.

The geological structure of the Ethiopian Highlands is very complex and results in a high variety of parent materials at the earth surface. The diversity is caused by the evolution of the East Africa Rift System, which started during the Precambriam (Berakhi et al. 1998, De Mûelenaere et al. 2012). In this study area, Precambrian metasediments and metavolcanics, which form the bedrock, are intensively folded and faulted and are unconformably overlain (indicating discontinuity in the stratigraphic sequence) by subhorizontal Paleozoic and Mesozoic sedimentary rocks. The oldest are known as Inticho sandstone and Edaga Arbi glacials and are exposed in several places throughout the region (Figure 3; left). This sedimentary succession dips very gently to the south and thickens southwards from less than 100 m in Eritrea to more than 500 m in Central Tigray (Kumpulainen et al. 2006). The Edaga Arbi glacials consists of 3 layers; a friable shale, a silty shale (mudstone) and tillite composed of fragments of metavolcanic rock and granite and gneiss boulders. Around Edaga Arbi, the total thickness of this layer is 200 m thick. The shale layers could have laminations of limestone and ice-rafted debris (Girmay 2006, Kumpulainen et al. 2006). The Mesozoic sedimentary rocks consist of Adigrat sandstone, a carbonate-marl-shale succession called the Antalo supersequence (Antalo limestone plus Agula shale) and another sandstone called the Amba-Aradam formation. The last formation is only found in the higher locations (2700 m a.s.l.) in the Mekelle basin, and will not be discussed further in this report. The Adigrat sandstone can be recognised by its prominent light yellow to pink colour. On top of this sedimentary rock, which in places are intruded by a network of dolerite sills and dykes, Tertiary lava flows (basalts) are found (Berakhi et al. 1998, De Mûelenaere et al. 2012, Nyssen et al. 2008, Van de Wauw et al. 2008, Tesfamichael 2010). Figure 3 gives a summary of this stratigraphic sequence and an indication of the spatial distribution.

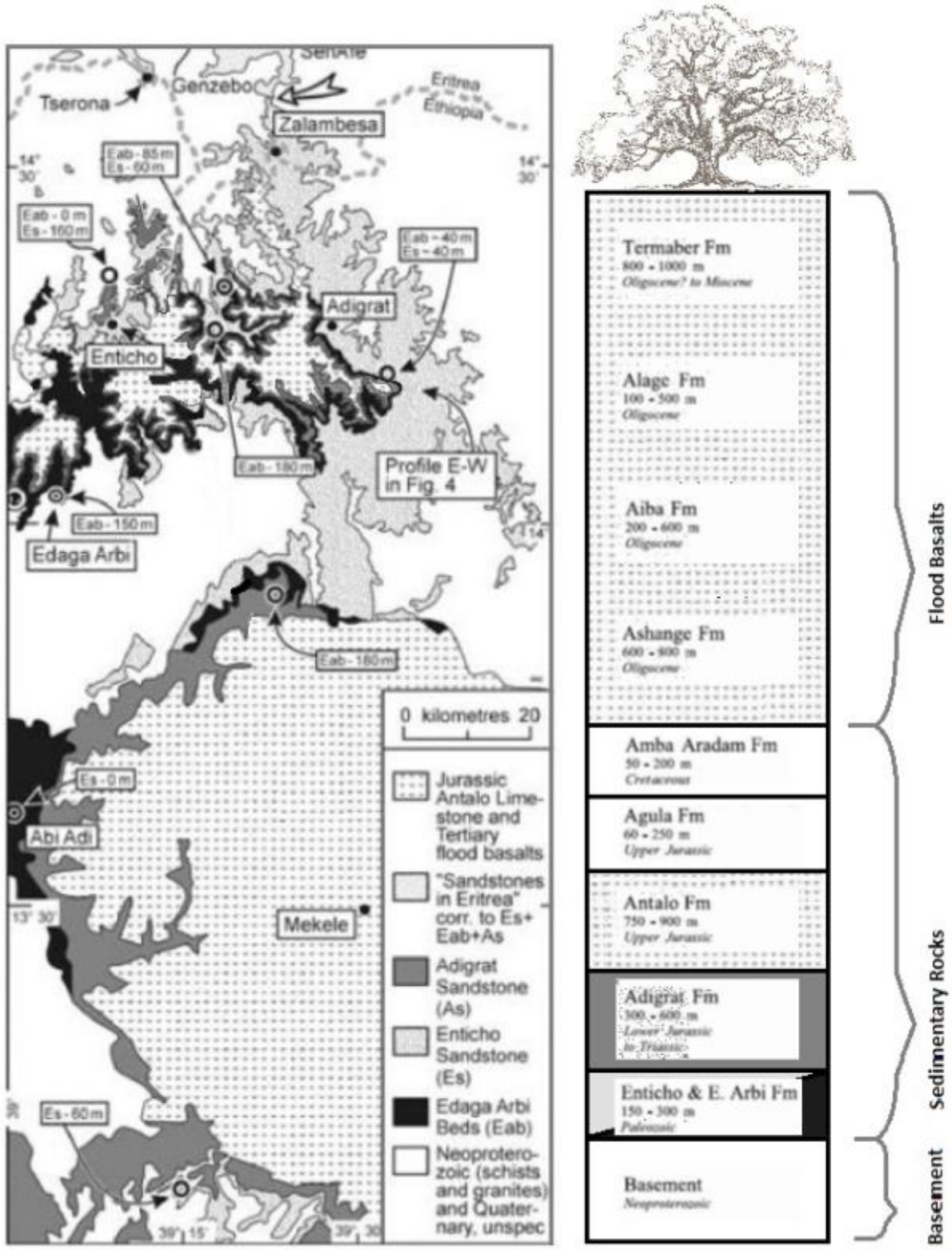

Figure 3: On the left: A geological map of the study area from Mekelle to the border with Eritrea. The thickness of the Edaga Arbi glacials and Inticho sandstone is indicated for some points (Kumpulainen et al. 2006). On the right: A schematic view of the stratigraphic sequence in the study area (Tesfamichael 2010). This particular layering has an emphasis on the Mekelle basin, which lays approximately 50 kilometres South-east of the Edaga Arbi study area.

Figure 4: Example of sedimentary rocks in the Northern Highlands of Ethiopia; According to the photographer, this shows Edaga Arbi tillites below Adigrat sandstone (Boon 2012). The greyish layer I recognise as the friable shale and the white layer as the siltstone/mudstone that we encountered around Edaga Arbi.

Figure 5: The typical step-like landscape with 'table mountains'; a canyon west of Adigrat in the Northern Highlands, Ethiopia (Houten 2002).

3.1.1.4 GEOMORPHOLOGY

Since the Oligocene, the most significant geomorphologic event started: tectonic uplifting of the Ethiopian Plateau started deep-reaching erosional processes, resulting in the step-like landscape that is characteristic of the entire study area (Figure 5). Flat summit surfaces are preserved (due to the lava flows on top), representing the remnants of the original 'plateau landscape' in the form of 'table mountains'. This typical morphology is caused by selective erosion of variable hardness, favouring softer rocks against harder rocks (Berakhi et al. 1998, Nyssen et al. 2004).

Quaternary continental sediments, such as alluvium, colluvium and tufa, can be found along the major river valleys, as well as in softly undulating areas and tectonic depressions (Berakhi et al. 1998, De Mûelenaere et al. 2012, Nyssen et al. 2004). Landslides and other mass-movements from the steep slopes are really important for soil distribution (Van de Wauw et al. 2008).

To distinguish different geomorphological elements, a quick aerial photograph interpretation of the Edaga Arbi study area was done. The digital version of the resulting sketch can be seen in Figure 6.

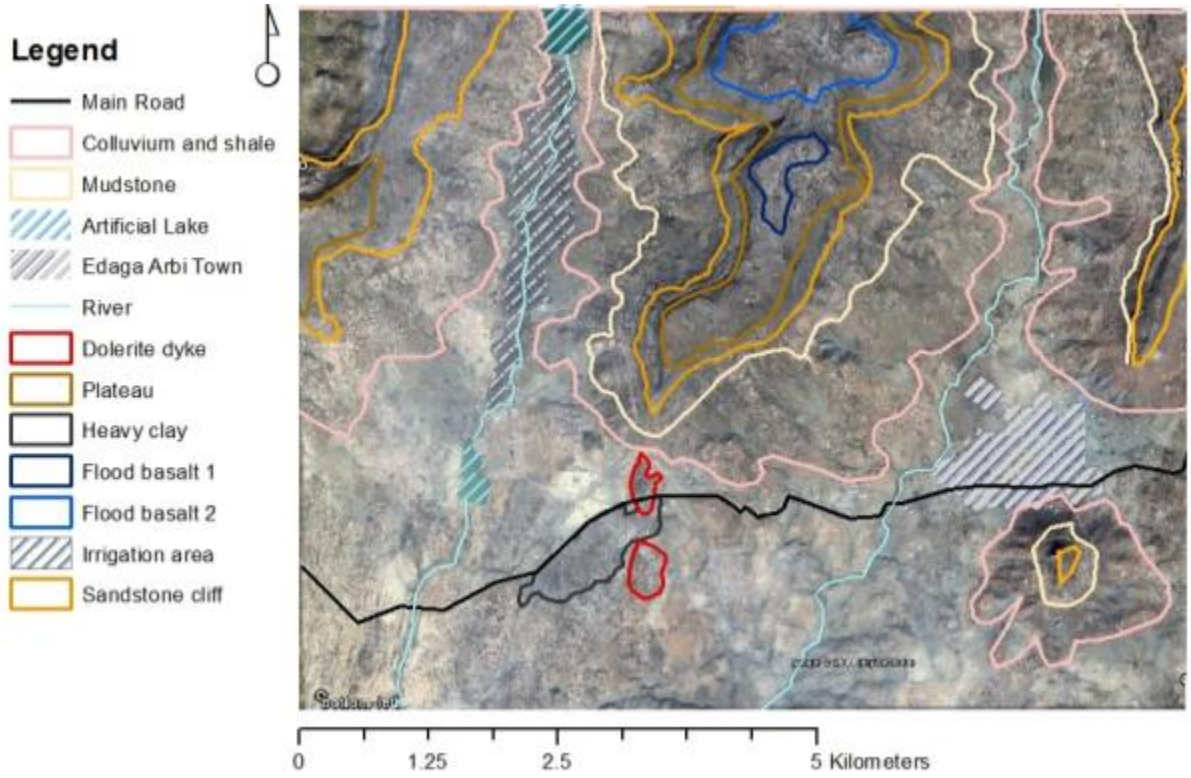

Figure 6: Aerial photograph interpretation on a surface of GoogleEarth (2013, December 13) imagery.

The most obvious landscape feature popping out of the aerial photograph is the sandstone cliff (in dark yellow), which is almost vertical and reflecting a light colour at the sunny side and a dark shadow on the other side of the mountain. On top of this another slope is present which includes a relatively flat surface. It could be the remnant of the old plateau landscape in which the sandstone rock has weathered in a typical subtropical laterite soil, this is mentioned to be present in the area by Girmay (2006). Typical laterite is porous and claylike and is formed under strongly oxidizing and leaching conditions. The colour is generally brown to red, because it is rich in iron oxide. But it could

also be one of the possible flood basalts. The blue lines indicates the flood basalts that lay on top of the plateau. This area could consist of multiple lithologies as described in the geology section, but based on this view it is unclear, as they show the same colour and land-use. The dark yellow line is again a boarder where a steep slope occurs. When zooming in on the picture (or GoogleEarth), a clear white line can be seen that is visible around the table mountain almost all the way around. This must be a geological divide of rock types. Between the sandstone cliff and the pink line, exists an area in which colluvium has been deposited on top of the Edaga Arbi Glacials. The underlying bluish grey shale is visible at the sides of deep gullies that cut away in the mountainside. In red, two hills that also pop up through the rest of the environment are delineated. The literature states that the sedimentary rocks are dissected by dolerite dykes and sills, maybe this is one. At last we have the black area south of the road with sticky heavy clay, this area clearly stood out amongst the more red hilltops (which are also in habit while the heavy clay is not). Both rivers cut thought colluvium and the underlying bedrock, the bare bedrock has a grey colour.

3.1.1.5 LAND USE AND -COVER

The original climax vegetation in the Highlands of North Ethiopia consisted of three types of vegetation based on altitude and moisture: Dry evergreen montane forest was present above 2200 m a.s.l., deciduous wooded grassland below 2200 m a.s.l. and mixed forest between an altitude of 1400 m and 2200 m a.s.l. in moister areas. Small remnants of these vegetation types can currently only be found around churches and in protected or isolated areas (De Mûelenaere et al. 2012, Girmay and Singh 2012). Under this (original) forest cover, thick organic layers can be found leading to Phaeozems (Nyssen et al. 2008).

At present-day, most of the vegetation is semi-natural (modified by human influence but retaining many natural features), consisting of cropland, degraded savannah, as well as non-indigenous species such as Eucalyptus (De Mûelenaere et al. 2012). To provide food for the household, farmers grow different cereals, peas, beans and lentils. Farm size in general is small; approximately 0.5-1 ha (Kraaijvanger et al. 2013, Nyssen et al. 2008) and the family size is large; an average of 5.2 persons in a rural family (USAID 2007). Crops are grown wherever it is allowed, which also include the shallow soils. In practice, most land with a slope of 30% and higher will not be used for agriculture and instead are established as 'area exclosures' in order to recover the biodiversity and soil quality, but there are exceptions, resulting in very narrow fields. The Eucalyptus is introduced in the form of plantations on degraded soils and generates income through selling the wood for fuel (Girmay, Singh. and Øystein 2010, Yami, Mekuria and Hauser 2013).

The agricultural production depends almost entirely on rainfall (Girmay et al. 2010). The first rainy season is important for the beginning of the growing season by deciding what crops to grow. Short-cycle crops, such as Maize, sorghum and finger millet, will be planted in March and depending on the success of the season, harvested in a secondary harvest season afterwards (in June or July). The second and main rainy season corresponds to the main *meher* growing season, in which wheat, barley and teff are grown. Both barley and teff crops are adapted well to the harsh environments in northern Ethiopia (Araya et al. 2010). During the hot and dry period, the *meher* crops will be harvested (in October and November). The soils are left bare during the rest of the dry season. Irrigation is not much implemented, although more and more regions construct artificial lakes by

building dams in sections of a river in order to save water for the dry period. Releasing water from these lakes, flooding fields, creates the opportunity to have another growing season.

Most of the understory vegetation (grasses and shrubs) is used for grazing of livestock (Girmay and Singh 2012), but also bare and harvested lands will be used for grazing. The livestock are an important status symbol and can be used as sources of cash, but are mostly used for ploughing (ox-drawn, locally called *maresha* (De Mûelenaere et al. 2012)) and to provide milk and farm yard manure which in turn is used for soil fertilising and as fuel for domestic use (Girmay et al. 2010, Kraaijvanger et al. 2013).

The human impact in the study area is an important explanatory factor of soil variability. The above mentioned land-use practices lead to decreased soil fertility, water erosion as well as tillage erosion. These processes result in frequent outcrops of saprolite (Regosols). On the other hand, human decisions like the exclosure policy rapidly lead to the formation of humus-rich topsoil (Descheemaeker et al., 2006). Also terracing with the use of stone bunds is extensively implemented, increasing soil quality and crop yields (Vancampenhout et al. 2006).

Summarizing; major land-use and land-cover types are respectively: open grazing, cultivated area, settlement, area exclosure, plantation and water body.

3.1.1.6 SOIL DEVELOPMENT

Van de Wauw et al. (2008) describe two soil catenas developed in respectively basalt and limestone parent material in the area of Hagere Selam. Also Nyssen et al. (2008), Nyssen et al. (2004) and Rabia et al. (2013) studied soil distribution in the Tigray Highlands. From these studies I found that, soil development and the resulting soil type are mainly dependent on topography, climate and parent material. Soil development follows contour lines of the topography. Land-cover and human practices, such as deforestation and tillage, play a supporting role. The common soil types in the region include Cambisols, Luvisols, Vertisols, Leptosols, Regosols and the occasional Phaeozem (Kraaijvanger 2013). Like said above, the Phaeozem is only found below old forest cover, of which not much is left. In contrast, the Cambisol and Regosol are the most dominate in the study area. These relatively young soils, had little chance for soil development due to soil erosion, which is a major problem with rain-fed agriculture. On the steep slopes (>30%), almost all soil has been eroded (also due to free grazing), which results in very shallow soils with a high rock fragment content. On the footslope of these steep slopes, colluvial material accumulates.

On the basalt parent material a typical red-black soil catena will be encountered. The red coloured soils are distributed higher and the black coloured soils are found on lower and flatter positions in the landscape. The red soil is a shallow and stony soil, e.g. a Chromic Cambisol on the shoulders (this is related to soil erosion and mass-wasting from this position), Chromic Luvisol on stable positions, or Chromic Leptosol in the case of severe erosion. The black soils are Pellic Vertisols which lay on the flat steps of the landscape, with impeded drainage due to an impervious rock type below. In between the red and the black soil, a transition zone exists in which the red colour and stoniness decreases and clay content increases gradually, leading to e.g. Vertic Cambisols. The lack of red hues is attributed to the poorer drainage in these positions (Van de Wauw et al. 2008).

The basaltic soil originating from higher in the landscape has distributed itself also downslope, covering most of the other parent materials. There are two processes involved: 1) Large scale mass movements (tens to hundreds of meters wide and hundreds to thousands of meters long) moved a lot of basaltic parent material downslope. The soils that are found on these large scale landslides form exactly the same catena as found on the in situ basalt: Skeletic Cambisols on the higher positions and Vertisols on the lower end. 2) Close to the foot of the sandstone cliff, black swelling clays, coming from creep-like deposits of Vertic soil material on top of the cliff form Vertic Skeletic Cambisols (Van de Wauw et al. 2008).

3.1.2 TRANSECT DATA

To relate the relationships found in literature, an additional dataset of field observations was collected in November 2013. This was done with use of transects over one typical landform (table-mountain). First the outline of this sampling scheme will be given, after this the procedures behind the measurements will be explained.

3.1.2.1 SAMPLING SCHEME

Because of limiting circumstances, we could only travel by foot inside a radius of approximately 10 km from the residence in Edaga Arbi. Within this area lays the Mymisham table-mountain. The most effective way of sampling would be to cross this land-unit by means of transects. Figure 7 indicates the approximate location and direction of the transects. With help of a guide, the environment was searched for farmers that would give permission to sample their land. It was not known beforehand which farmer or what field we would sample, this was random as long as they were located near to the planned transect. The first transect covered the Mymisham table-mountain in a direction from West to East including each catena position with one point observation. This meant starting with the valley position on the other side of the mountain, continuing up with lower-slope, middle-slope, upper-slope, top. Those last two positions were in an area exclosure and unreachable. The transect continued down to the other side (Figure 8); top, upper-slope, middle-slope, lower-slope and valley position. The second transect was taken in the direction beginning from the top of the plateau to the lower plain in a general North to South direction trying to include points with slight relief differences. The Northern direction was not sampled, because it showed no big elevation differences. The transect dataset resulted in a total of 14 point observations which lay in a zone of approximately 500 m around the line.

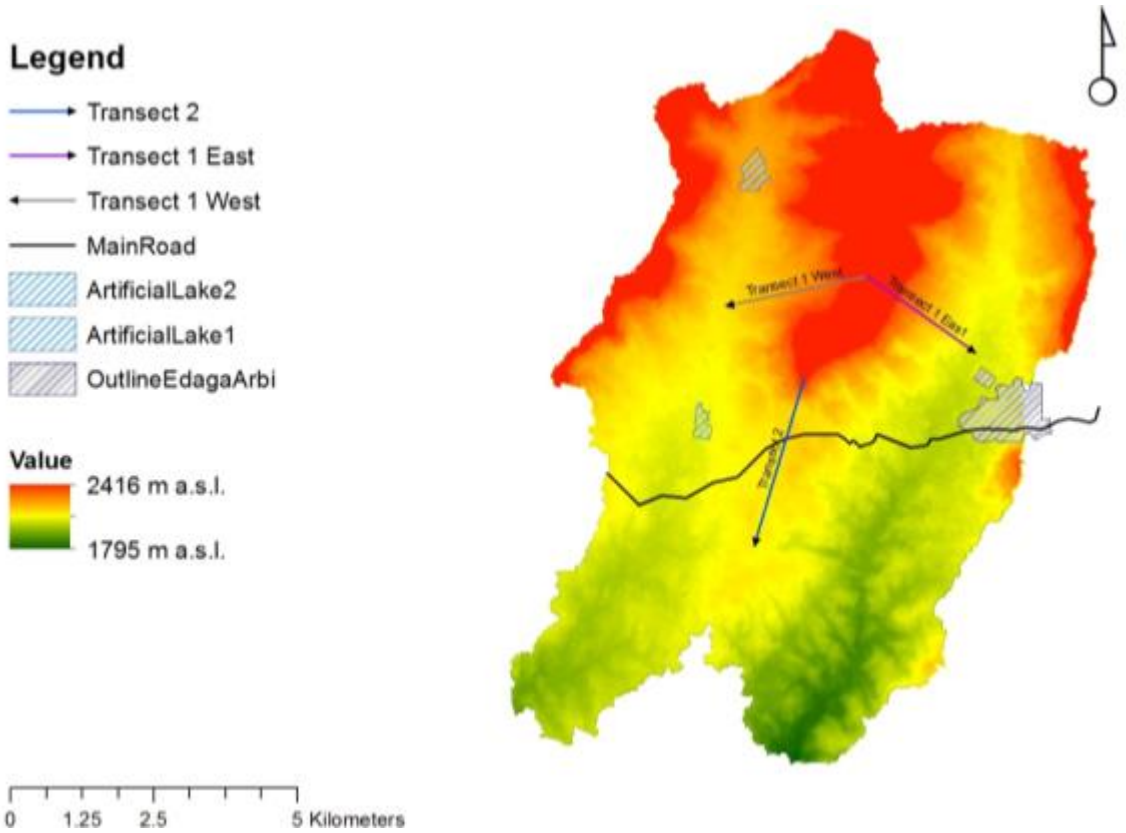

Figure 7: The location of the transects over Mymisham (1) in a West to East direction and into Zonghi (2) in a North to South direction, on top of the digital elevation model.

3.1.2.2 MEASUREMENTS

For each of the observation locations a soil profile description, according to the FAO guideline to soil description (FAO 2006), was made resulting in a soil type with qualifiers according to the WRB. This included a general description of location, topography, geomorphology, land-use and management practices. Soil classification was mostly done by drilling with use of an auger of 90 cm, but in the case of many stones or a massive soil layer, a pickaxe was borrowed from the farmer and a profile pit was dug up to a depth of 50-60 cm, or a pit was located near to the field. At each location, some photos were taken of the soil profile and the environment, with the purpose of future reference. In addition, bulk soil samples were taken of the topsoil (the first 10 cm of the profile) and, if possible, the subsoil (on an approximate depth of 40 cm). The topsoil samples were tested with use of our 'portable soil lab' for pH, nitrate, texture, soil colour and lime. The subsoil was checked for signs of clay illuviation, and tested for texture and lime. Preparation of the soil included crushing of aggregates and sieving with a (almost) 2mm sieve, removing plant material, stones and gravel.

For the pH measurement, a soil solution was made based on 1 part soil and 10 parts demi-water (0.5 Tbsp soil with 5 Tbsp of water). This was shaken for 5 minutes and then measured with a portable 18.52.SA multimeter with an electrode.

Figure 8: Scope of the East side slope (transect 1, east) of the Mymisham table-mountain from the river Mayira upwards. The person waving stands on top of slate bedrock. Also clearly visible is the sandstone cliff in the distance (own work).

The nitrate content was measured from the same soil solution with nitrate-test-strips and a nitracheck 404 reflectometer with its corresponding procedure (Eijkelkamp 2004). Soil texture was derived in two ways, first by the procedure of the FAO for field estimation and second by the procedure of Stoorvogel, Hendriks and Claessens (2013) with use of a turbidity meter; Turbidimeter Turbicheck AL250T-IR. This device measures the intensity of the, by the sample (in solution), scattered light. The solution consisted of 0.5ml (1/8 teaspoon) soil and 100ml tap-water and is measured after 40 seconds and one hour. The resulting values have to be calibrated with laboratory measurements (in the Netherlands) to determine the texture fractions. For this purpose 15 different soil samples had to be taken to the Netherlands. Unfortunately, these were reported missing, so these calibrations could not take place. The texture measurement by the method of Stoorvogel et al. (2013) was therefore not used in further analysis.

Soil colour was determined with use of the Munsell soil colour scheme (moist conditions). The presence of lime was tested with a HCl solution; bubbles indicate a lot of lime (2), some bubbling noise for some lime(1) and no reaction indicates no lime present in the soil (0).

In case of the SOM fraction of the soil, this could be roughly estimated in two ways. The first method is based on the Munsell soil colour 'value' and 'chroma' properties and texture observations following Table 46 (page 43) in the FAO guideline (FAO 2006). The problem is that this estimation is strongly dependent on different type of clay minerals leading to darker and lighter coloured soils and the fact that the SOM content tents to be overestimated in dry soils, such as the ones in the study area. The second method of estimation is using the nitrate measurements. This calculation is in turn

based on the soil texture, an estimated bulkdensity (derived for each individual sample from profile structure type and grade), the fact that nitrate (the available part) is commonly only 2-3% of total nitrogen in the soil, an estimated C:N ratio of 12 and the notion that the SOM commonly consist of 58% carbon. The results of the measurements and various observations were collected and analysed for variability.

3.1.3 DATA LAYERS AND TOOLS

In preparation to the study, shapefiles with administrative boundaries in Ethiopia were collected. These are used as 'cookie cutter' in delineating the approximate study area. The files are freely available for download in the GADM database of Global Administrative Areas (GADM 2012).

Conform with the SCORPAN model (McBratney et al. 2003), an inventory of available data layers was drawn up that could describe the soil forming factors trough landscape or terrain attributes. As suspected this availability was limited, as it only included detailed information on topography and vegetation leaf reflectance. One of the main soil forming factors in this study area is parent material, which was not available in the scale and quality needed. However, differences in parent material mainly express themselves in various geomorphologic units which can be read from differences in topography and its derivatives like slope.

For the basis of this geomorphology map the ASTER GDEM (the Advanced Spaceborne Thermal Emission and Reflection Radiometer), with an approximate resolution of 30 meters was used. ASTER GDEM is a product of METI and NASA (2011). The global extent was cut to the extent in Figure 2. From this surface different derivatives can be studied, e.g. slope, aspect, curvature and flow accumulation as explanatory variables explaining the soil variability.

The vegetation data is available through multispectral imagery from the U.S. Geological Survey (2005), in a 30 m resolution. The NDVI (Normalized Difference Vegetation Index) is a ratio calculated from the spectral reflectance measurements in the visible (red) and near-infrared regions:

$$NDVI = (NIR – VIS)/(NIR + VIS)$$

Negative values will represent non vegetated areas which have a rather low reflectance in both spectral bands, such as free standing water (lakes and rivers). Increasing positive values represent increasing vegetation density. The images are taken in the beginning of the dry season (approaching harvest time with ripening crops), because at this time the vegetation shows the clearest distinction between 'semi-natural' and agricultural vegetation.

These collected data layers are read, analysed and classified in the ArcGIS environment (ArcMap and ArcCataloc) version 10.1 (ESRI, 2012). A flowchart of the taken actions, calculations, used tools and the raster output can be seen in detail in Figure 9.

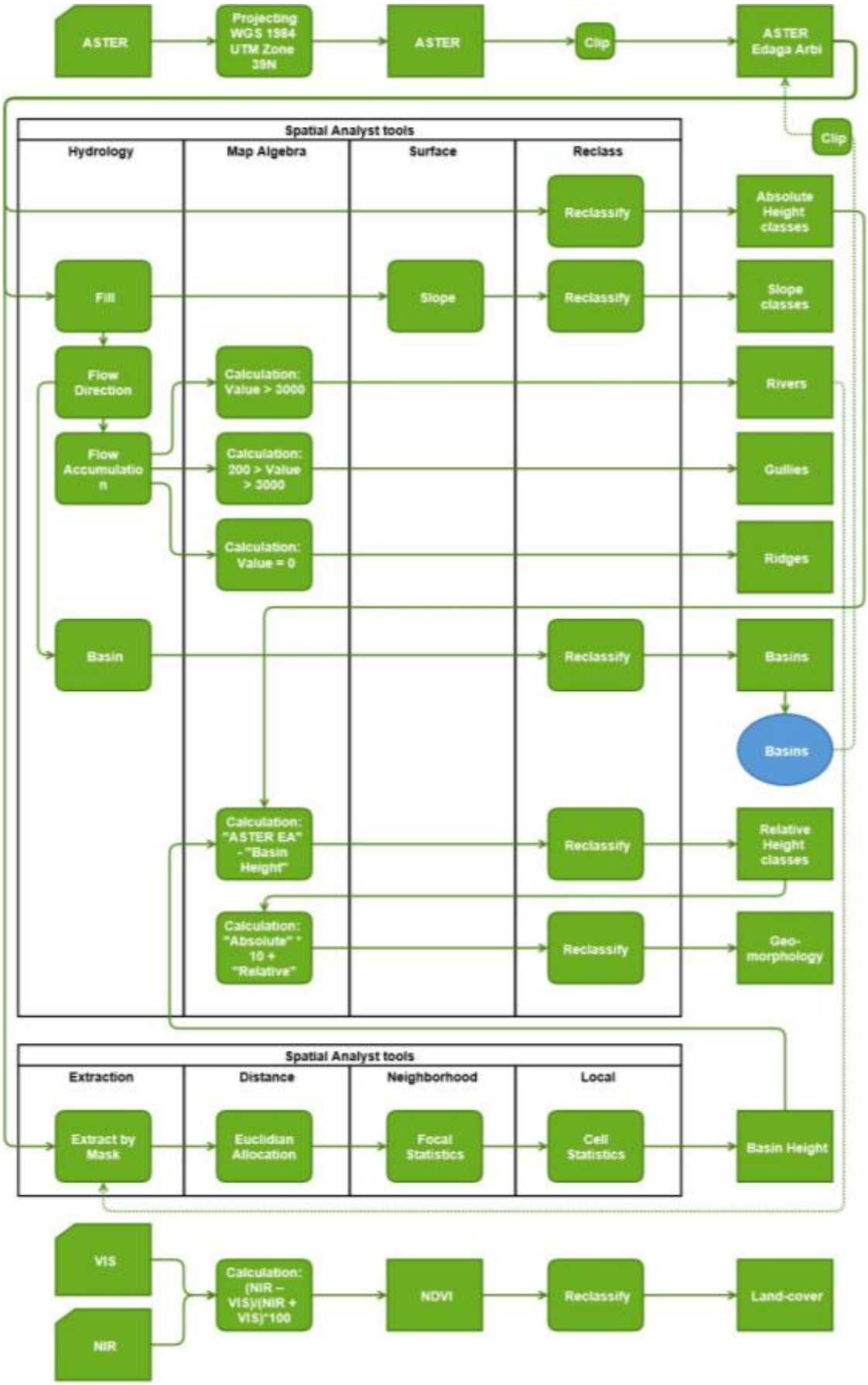

Figure 9: Flowchart of used tools and procedures in ArcMap.

A study of the absolute height, in combination with the (geomorphological) understanding developed in the previous sections, resulted in the approximate distribution of the rock types at the surface in the area. The classification was done with the Jenks natural breaks optimization method in 7 classes. This optimization method seeks to minimize each class's average deviation from the class mean, while maximizing each class's deviation from the means of the other groups. In other words, the method seeks to reduce the variance within classes and maximize the variance between classes. In practice this means for the topography classification that the classes are boarded at places with steep slopes, exactly where geomorphological boarders lay (this is confirmed by the aerial photograph interpretation). In addition, the relative height is calculated; a layer corrected for the descending of the two rivers. The Seysa river lays somewhat higher in the landscape than the more incising Mayira river (Figure 7) and this influences the grade of erosion through the different gradient. The method behind the calculation (Figure 9) is the following: for each basin the location of the river was calculated. These cells then got the value of the altitude assigned to them. This 'river height' raster was then used to extrapolate these values to the whole area of the basin, resulting in a smooth 'basin height' raster. This was then subtracted from the original DEM, resulting in the relative DEM. This raster was also classified with the Jenks natural breaks optimization method and studied. The decision was made, based on the aerial photography interpretation, that only the area closest to the river (up to 25 m) made sense as an individual geomorphological unit. The resulting classified absolute and relative elevation rasters were combined into the geomorphology map. Additional derivations of the DEM, such as slope, aspect and ridges were also classified and will be analysed as possible explanatory variable for the soil development.

The classification of the land-cover map is based on the NDVI data with a Jenks natural breaks optimization method in 8 classes. Identification of the land-cover was based on the location in reference with what was seen on the google image. This meant that some classes were merged to one, when no difference was spotted.

3.1.4 THE DECISION TREE MODELS

As Figure 9 indicates, various rasters were calculated and classified in order to serve as possible explanatory variable to soil type, texture and organic matter content. To map the distribution of these different soil properties and types, different decision tree models will be made (one for each target variable). The rules of the model structure will be based on the knowledge of the general relationships found in literature, the transect data and the classifications of the available explanatory variables from the auxiliary information layers. The differences between each class are maximized due to the Jenks natural breaks optimization method. First the most explicit explanatory variable will be selected to form the first branching sequence. Then a second will form a second branching sequence, leading to a more detailed view of the situation. At last a third branching sequence will lead to the predictions of the target variable.

3.2 MODEL VALIDATION

The validation of the decision tree models requires an independent dataset of point observations. How these are collected is explained in Section 3.2.1.1. The validation data will be used to test the accuracy of the resulting maps (Section 3.2.3) and also to evaluate fractions of explained variance by each explained variable in the decision tree's classification structure (Section 3.2.2).

3.2.1 VALIDATION DATA

3.2.1.1 SAMPLING SCHEME

Before the actual development of the maps, soil data from sample points in the Edaga Arbi study area were taken with use of a stratified random sampling scheme (Figure 10). The study area of Edaga Arbi was divided in four strata; the first divide was based on the North to South transect and divided the area in an East and West side. The next taken divide was the approximate site of the main road that crossed the area from West to East, laying below the table-mountain. This divided the area in North and South, with the North being "close" to the table-mountain and the South being "further away" or like upstream and downstream. Each strata should contain at least five sample points, but due to accessibility and travel distance the most points were taken in the North-East strata. In total 34 sample locations were visited in the Edaga Arbi region of which 2 lay outside the rivers influence (basin area); those were not used in further analysis.

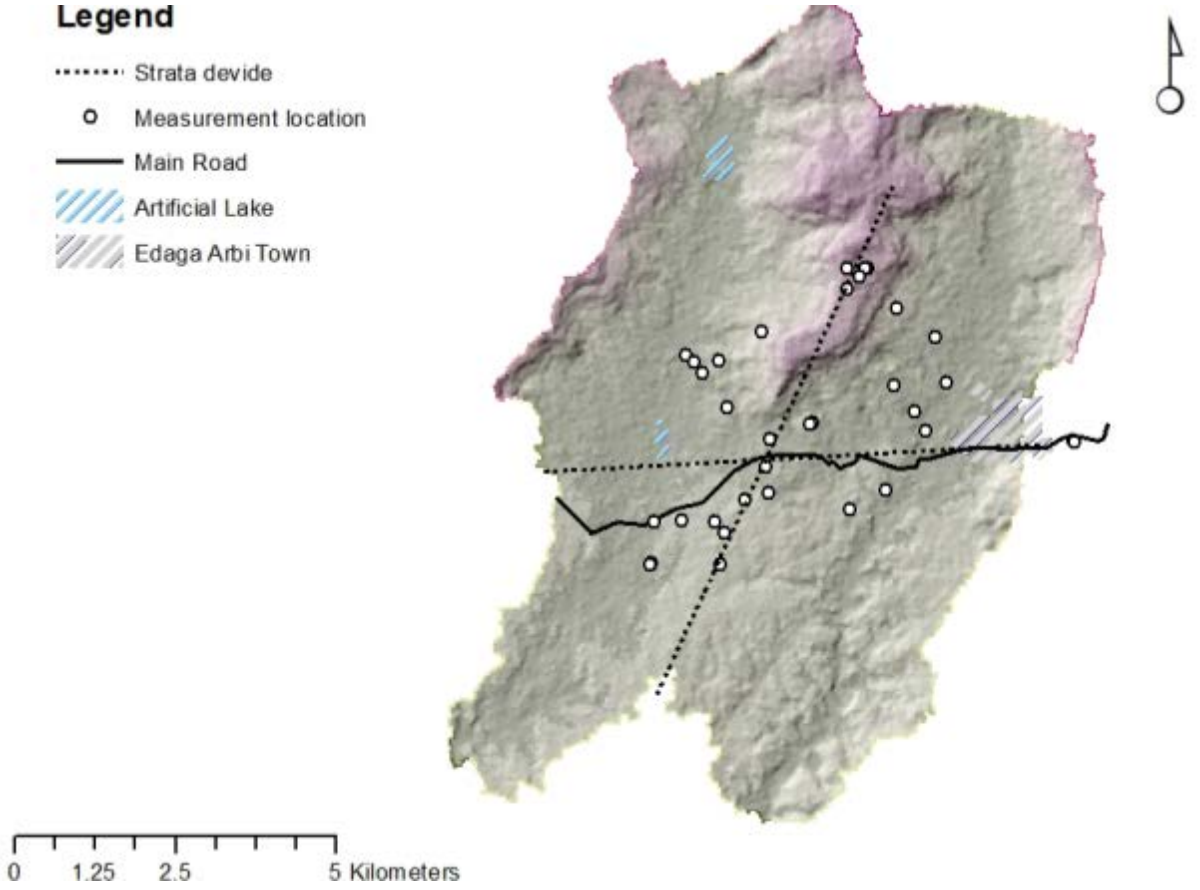

Figure 10: Measurement locations and strata in the Edaga Arbi area for validation. The table-mountain is in purple, while the lower area is in gray tones due to a hillshade layer.

3.2.1.2 MEASUREMENTS

Samples of bulk top- and subsoil were taken from the sites and the same amount of soil profile classifications were done on site. Soil classification, sample measurements and gathering of environmental information followed the same procedures as earlier with the transect data-gathering (Section3. 1.2.2).

3.2.2 ANALYSIS OF THE DECISION TREE

With the analysis of the decision tree, the fractions of explained variance are calculated per explained variable that could predict the target variables. In other words, each of the classification steps in the decision tree are evaluated for explained variability.

In the analysis of variance (ANOVA), one calculates three different sums of squares (SS), namely total sum of squares (SST), between group sum of squares (SSB) and within group sum of squares (SSW). These values are then compared in fractions. The fraction of explained variance, or the coefficient of determination (R^2) is the square of the sample correlation between the variables, and:

R^2 = explained variance / total variance = SSB / SST

When the variability between groups is small, then the groups are very similar and the classification is not sufficient or necessary. So this variability needs to be bigger in order to prove the impact of the classification and to test for this, a F-test is preformed:

F = explained variance / unexplained variance (residual) = SSB / SSW

The resulting fraction has to be compared to a value in a table of critical F values on significance level of $p < 0.05$ and depends on the degrees of freedom of the total data-set and the sub-sets (classifications).

3.2.3 MAP ACCURACY

This assessment will be summarized in a confusion matrix in which the difference between model output and ground truth is displayed. From this we can derive the total-, producers- and users accuracy.

3.3 MODEL EXTRAPOLATION

After the model development and a successful validation in the local area, the next step is to extrapolate the model to the extending landscape. First the similarities and differences between the Edaga Arbi modelling site and the extrapolation sites need to be analysed (Section 3.3.2), in order to check the assumptions that were made during the geomorphology classification. The extrapolation dataset (Section 3.3.1) was collected prior to checking the representability and is used to validate the soil variability map in one of the representative areas chosen from the extrapolation sites (Section 3.3.3).

3.3.1 EXTRAPOLATION DATA

In order to assess the accuracy of the extrapolation a small extrapolation dataset was be collected, which will consist of clusters of random points. The clusters, or extrapolation sites, are located around the main towns of the other woredas (Section 3.1.1), respectively Hawzen (HW), Inticho (IN) and Hagere Salam (HS).

3.3.1.1 SAMPLING SCHEME

For convenience, we travelled with Richard Kraaijvanger to the locations of his 16 study sites, four agricultural fields in each woreda. This was done in October and November 2013. The fields were forwarded by his farmer groups and needed to be harvested (for his research purposes). During the process of harvesting, the soil got available for soil drilling and classification. When the right opportunity was met (permission of farmer, harvested or fallow cropland, time) then an additional field was visited of the same tabia. This resulted in 8 plots in Hawzen, 5 in Inticho, only 3 in Hagere Salam (because harvesting was only possible for 2 fields). This sampling scheme is best described as semi-random, because it was not beforehand chosen, but it excluded the areas in which Mr. Kraaijvanger did not have any connections.

3.3.1.2 MEASUREMENTS

Samples of bulk top- and subsoil were taken from the sites and the same amount of soil profile classifications were done on site. Soil classification, sample measurements and gathering of environmental information followed the same procedures as earlier with the transects and Edaga Arbi validation samples (described in Section 3.1.2.2).

3.3.2 AREA REPRESENTABILITY

The representability of the regional study area (blue square, Figure 2) in relation to the local area (EA) must be analysed, because these must be similar in such a way that the rules in the decision tree can be directly transferred to the outer area. To study the accuracy of the model in the extrapolation area, a smaller representative area is selected from within (like the Edaga Arbi Study area, the boundaries of the extrapolation test area are determined by a basin analysis). Possible locations taken into account are the following extrapolation sites; Hawzen (HW), Inticho (IN) and Hagere Salam (HS). For this purpose, no observations were available, so this consideration is based on literature, expert knowledge and GoogleEarth reference images.

From the literature it became clear that there are discontinuities in the stratigraphic sequence (Section 3.1.1.3). This fact affects the model in its first stage when transforming the topography data in geomorphologic categories. For example, the rules for the classification of geomorphology are based on the assumption that the layering of the rock types were practically horizontal and of constant thickness. For this local scale it was a valid assumption, but it needs to be confirmed for the other areas before extrapolation. In the case of incorrect assumptions, one would examine modifications to the model or the surface data input.

For each possible extrapolation site, one should look for the same geomorphologic units. The most obvious one would be the ‘finger-shaped’ table-mountains, topped by flood basalts, which will be clearly lined by a sandstone cliff. You can see such a feature around Inticho (Figure 11). This town lays approximately 25 kilometres to the North from Edaga Arbi.

Figure 11: GoogleEarth image of Inticho and surroundings. Relatively flat terrain with distinctive cliffs surrounding it indicate remnants of the plateau landscape. The valley has a light colour, clearly distinguishing itself from the red plateau and the dark flood basalts.

The Hagere Salam area, which lies approximately 50 km to the South, does show the same landscape with table-mountains, but has an additional step (has higher altitude) and contains limestone (Van de Wauw et al. 2008, Tesfamichael 2010, Nyssen et al. 2008). The relationships explaining the soil variability on these geomorphological units are not implemented in this soil-landscape model, because they were not present in the Edaga Arbi region. For the second area, Hawzen, which lies approximately 40 km to the East, there are no 'fingered' table-mountains that are cut by a network of gullies and rivers. The landscape can be better described as a big plateau with a cliff. It is the most northern part of the Mekelle "plateau". The soil has a more sandy texture and a light colour, which resulted from a different parent material on the surface. This is most probably Adigrat sandstone, which is described by Rabia et al. (2013) to be present at the northern border of the plateau.

So, two of the areas that were visited during the excursions, are too different from the Edaga Arbi region. Those discontinuities are caused by a fault system that is encountered South, South-East of Edaga Arbi. The assumption of horizontal layering and constant thickness of the rock types is invalid when going from Edaga Arbi to the South and/or East. In addition other parent materials are encountered. Therefor these extrapolation sites (HW and HS) are not suitable for extrapolation.

However, the Inticho area does show potential, although some minor corrections need to be applied. For one, literature dictates that in a Northern direction, the Edaga Arbi glacial deposits change halfway, somewhere beneath the overlying Adigrat sandstone, to Inticho sandstone. Also the thickness of both the glacial deposits and the Adigrat sandstone is observed to decrease when moving to the north (Kumpulainen et al. 2006). Overall this decline in thickness is estimated to be 100 m over 25 km (0.4 %) based on picture interpretations (Figure 12).

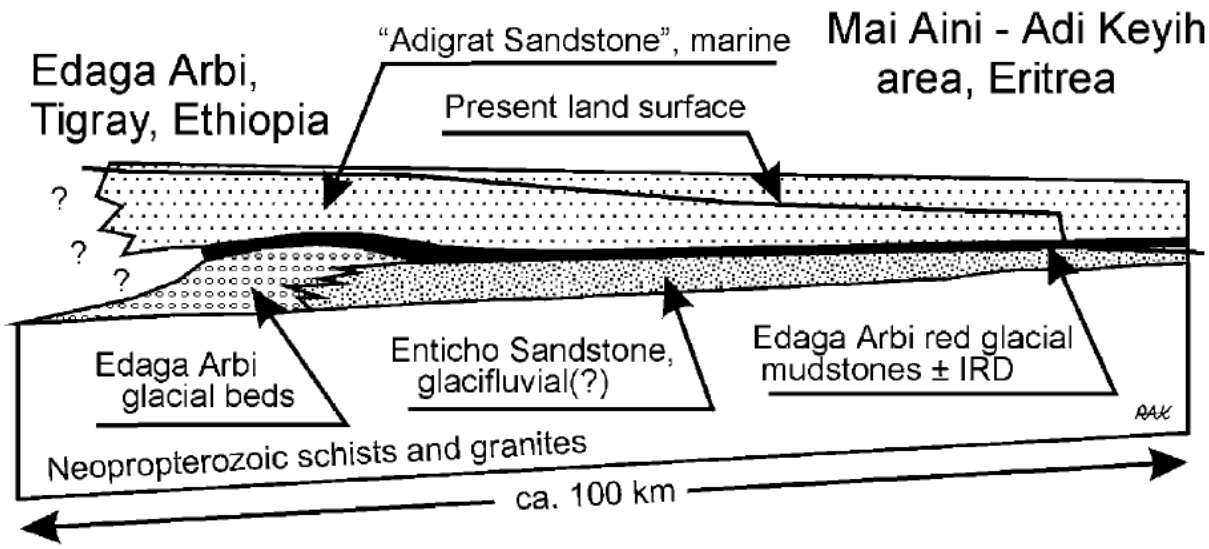

Figure 12: Geological profile from Edaga Arbi to the North according to Kumpulainen et al. (2006).

This decline in thickness can be corrected by creating a surface that linearly increased in height in the direction of Edaga Arbi to Inticho (South to North). The raster surface is added to the original ASTER surface, correcting for the small decline. This way one can assume the rocktypes are stacked horizontally again, and the same heights as in the Edaga Arbi region can be used for classification of the geology and geomorphology. The method for creating this raster surface is the following: first a point feature dataset covering the whole area of interest needs to be created. This was done in a raster structure; each point in the centre of a raster cell. Then each point was assigned a 'height value' ranging from -25 to 150 according to the location of the point (the values 0 and 100 were on the lines of Edaga Arbi and Inticho respectively). This point feature dataset was then interpolated to a raster surface (with the same cell size as the ASTER DEM, this is important in further analysis) using IDW.

The geomorphology classification and decision tree-models can be directly copied from the Edaga Arbi region, to be implemented in Inticho after this small correction. The other explanatory raster data layers, such as slope, aspect, ridges etc. are made according to the same procedure as described in Section 3.1.3. This will be used to predict the spatial distribution of soil type, texture and/or SOM depending on the previous validation

3.3.3 ACCURACY ASSESSMENT

Because of the very limited amount of observation points per extrapolation site (Section 3.3.1.1), it is not possible to assess the accuracy with a confusion matrix. Instead a normal table will be shown to directly compare the modelling outcome with the ground truth data.

4 RESULTS AND DISCUSSION

This chapter consists of three steps with the results of the model development and application (Section 4.1), model validation (Section 4.2) and the model extrapolation (Section 4.3)

4.1 MODEL DEVELOPMENT AND APPLICATION

The relationships defining the local soil variability in the Northern Highlands of Ethiopia will be determined and implemented in three decision tree models (Section 4.1.4). These are based on the conclusions of the literature study (Section 4.1.1), the results of the transect survey (4.1.2) and the classification of the auxiliary information (Section 4.1.3).

4.1.1 LITERATURE STUDY

The main soil forming factors in the overall study area of central Tigray, are considered to be parent material, topography and climate (Section 3.1.1.6), so these will be the main factors taken in consideration in the classification of the available auxiliary information. The literature only provided information on relations that were specifically for the HS area. Although this is a similar area as EA, it applicability needs to be confirmed. The additional data will also provide a more detailed view.

4.1.2 TRANSECT DATA

From our observations (Table 1) we can conclude that the percentage of surface stoniness in the area is relatively high with a mean and sd. of 56% and 19% respectively. One location on the high plateau hit 85% in contrast to the lowest amount of 25% in the river valley. The surface stoniness is related to the next observation of the content of stones in the soil profile, which decreases right below the surface. This is due to a tillage induced mechanism that turns the soil upside down and mixing it, bringing the stones from below to the surface. The finer soil fraction of the loosened soil then fills the pores (during rain), but the bigger stones stay 'floating' on the surface.

The Munsell colour hue is not included in the table, but the observations indicate that it is mostly 10YR for the somewhat younger soils and 7.5YR for the slightly older soils. The typical tropical bright red colour (5YR) was only found once during the transect measurements. Values were relatively light and the chroma moderately bright leading to a moderate to low SOM estimation. Based on the literature, this findings are representative for the rest of the study area.

The pH results are strikingly similar for all locations with a mean of 7.3 and a sd. of 0.24. This is not in agreement with measurements of Kraaivanger (2013), who found a slightly acid pH in the range of 4-6 with the use of a different method. This data showing lack of variability could be explained by the field measurement procedure that is different from laboratory analysis. For one, the demineralised water was contaminated resulting in a pH of 2.5. Because of this unreliability of the bought demi-water, we choose to use tap-water, although the minerals it contains could have buffering properties.

The nitrogen content is measured to be relatively low, this is as expected although it should be noted that these values are not calibrated with laboratory measurements, and could therefore be untrustworthy. The SOM content that was estimated from the nitrate measurement shows the same

order of magnitude as the other estimation method using soil colour, more precisely, the mean and standard deviation of both SOM measurements are the same, which could suggest a correlation and point to the fact that the assumptions made in the calculations of both values are correct. However, when plotting both figures against each other, no relation is found, so this can be seen as a coincidence.

Table 1: Measurement results, mean and standard deviations of various soil properties from the transect sample points. The clay content is an estimated range based on the observed texture class, conform to Table 25 in guidelines for soil description (FAO 2006).

Site-nr.	Surface Stoniness [%]	Munsell Value	Munsell Chroma	Munsell SOM [%]	pH	Nitrogen content [%]	SOM from N [%]	Clay Top [%]	Clay Sub [%]
EA004	60	4.0	4.0	0.6	7.1	0.10	2.1	25-40	40-60
EA005	85	3.0	2.0	3.0	7.2	0.11	2.2	25-40	>60
EA007	25	3.0	3.0	3.0	7.1	0.09	1.8	40-60	40-60
EA008	80	3.0	4.0	1.5	7.2	0.19	3.8	>60	>60
EA009	70	3.0	2.0	3.0	7.4	0.08	1.7	>60	>60
EA010	40	2.5	2.0	4.0	7.1	0.15	3.1	<12	<10
EA011	30	3.0	2.0	3.0	7.1	0.10	2.0	25-40	-
EA012	60	3.0	2.0	3.0	7.2	0.19	4.0	>60	>60
EA013	70	3.0	2.0	3.0	7.7	0.17	3.6	>60	>60
EA014	50	3.0	1.0	3.0	7.5	0.04	0.9	>60	>60
EA015	30	3.0	1.0	3.0	7.8	0.09	1.8	>60	>60
EA016	60	3.0	4.0	1.5	7.1	0.19	3.9	25-40	40-60
EA017	75	3.0	3.0	3.0	7	0.10	2.1	25-40	25-40
EA018	50	3.0	4.0	1.0	7.2	0.11	2.3	10-25	-
Mean	56	3.0	2.6	2.5	7.3	0.12	2.5	38-56	44-62
SD	19	0.31	1.1	1.0	0.24	0.047	1.0	24	22

The texture in the area consists mostly of clays and loams, with a high amount of heavy clay soils (6 out of 14). One could also see from comparing the clay content of the top- and sub-soil, that for some of the plots, the clay-fraction somewhat increases with depth. The overall relation that can be drawn from the transects is that the texture on top of the basalt flow consists of heavy clay, which changes to a coarser texture (mixed clays and loam) on the slopes to finer textures like heavy clays in the valley position. One thing should be noted though, that is the location right underneath the sandstone cliff which also contained a heavy clay texture. These relationships were also found by Van de Wauw et al. (2008). In case of the SOM distribution, the younger soils, in principal, will have less build-up of organic carbon (SOC) than the older soils.

The main soiltypes that were found, include the following soil types; Leptosols, Vertisols, Luvisols, Cambisols and Regosols. Based on own observations (and the reference pictures), complemented with knowledge from Tesfamichael (2010) and Van de Wauw et al. (2008), a schematic of the resulting soil catenas and the proposed geological setting can be seen in Figure 14 and 18. The geology is based on the literature and multiple picture interpretations like the one in Figure 13. In the Mymisham transect the geology comes best to light at the sides of gullies and at the river. This is because of the large gradient in the area and the erosional power the water has during the rainy season (Figure 15).

The basement is made up out of a dark blue rock with quartz veins (Figure 17, left). The quartz veins develop under high pressure and are therefore typical in metamorphic rock. The colour is similar to that of basalt, concluding this rock could be metavolcanic. On some places the rock forms sharp peaks, pointing vertically; strongly tilted slate (Figure 8). Locally, when following the river upstream, a thick layer of colluvial soil is established on top of this bedrock (Figure 14f). It is more likely that this soil is deposited by a colluvial mechanism, such as sheet wash during rain storms, than by river flooding, because it is only the beginning of the stream and clearly has too much of erosive energy to be depositing sand and clays (Figure 15). Within this deposit, distinct layering of different textures, gravel and non-rounded boulders can be seen.

A little higher in the landscape, at the site of recent landslides, a bluish to grey shale deposit is found that crumbles really easily into small platy flakes. You could also clearly distinguish some thin out sticking layers between the shale, these layers have another texture and could be limestone or siltstone, but this was not verified. I consider this must be the Edaga Arbi shale (Figure 16). I assume the (brown) Vertisol (Figure 14a, Table 2; EA007) developed in this deposit for a number of reasons: 1) the heavy texture could be from this friable shale; 2) the influence of the river flooding is only recent (for irrigation purposes), ruling out a very thick layer of alluvial deposit; 3) the colour is much lighter than the other clays found in the area, which originate from the basalts. Somewhat higher in the landscape (+/- 6 meters) another clay soil was found, this time a bright red Luvisol with a high amount of surface stones (Table 2; EA008) of both basalt and sandstone. This points out to a colluvial origin after all.

Much of the Mymisham slope was an unstructured mix of colluvial material leading to much different textures and having both basalt and sandstone boulders (Figure 14b, Table 2; EA009). Halfway the slope, above the shale, a layer of white mudstone or siltstone was visible (Figure 13). This was tested with HCl, but showed no signs of calcium, ruling out limestone. Right below the sandstone cliff, on the East side of the mountain, a local dark heavy clay soil was found with big cracks (Figure 14e and 17, right). Like Van de Wauw et al. (2008) found, this could be a mass movement of vertic clays originating from the flood basalt on top of the mountain. This location was also the only location were the soil reacted strongly to the HCl solution (Table 2; EA013). Since limestone was not likely to be present, another possible explanation could be travertine. This is a form of limestone deposited at the sites of mineral springs. Such a spring was very close to sampling point. The tillite, that is expected on top of the mudstone and below the sandstone, did not come to the surface in this transect, most probably because it was overlain by colluvial material originating from above.

On top of the plateau, above the sandstone layer, a variety of bright red mixed sandy to clayey soils developed (Figure 14, Table 2; EA005). The texture differs on a very small scale (per field) and could be explained by terrace building and other management practices, but also local mass movements. Going up the flood basalts, it was very prominent that all level surfaces were dark coloured Vertisols (Table 2; EA012). However, on the crest (Figure 14c, Table 2; EA011), the soil was too shallow and classified as a vertic Leptosol.

Table 2: Profile descriptions of the transect points. Abbreviations are according to the FAO guideline to soil description (reference); L = Loam, SiC = Silty clay, C = Clay, SCL = Sandy clay loam, HC = Heavy clay, SL = Sandy loam, CL = Clay loam, SC = Sandy clay, SiL = Silty loam; GR = granular, SB = sub-angular blocky, SG = single grained, MA = massive, WE = weak, MO = moderate, ST = strong, VF = very fine, FI = fine, ME = medium, CO = coarse, VC = very coarse.

Site-nr.	Horizon	Depth [cm]	Munsell Colour	Texture Class	Structure (type, grade, size)	Stone Content [%]	HCL
EA004	Ap	0-20	10YR 4/4	L	GR MO FI	30	0
	Bw1	20-50	7.5YR 4/4	SiC	SB ST ME	5	
	Bw2	50>90	7.5YR 5/4	SiC	SB ST ME	40	
EA005	Ap	0-15	5YR 3/2	C	GR WE FI	10	0
	AB	15-35	5YR 3/2	C	SB ST ME	5	
	Bw1	35-50	2.5YR 3/3	C	SB ST ME	0	
	Bw2	50-80	5YR 3/4	SCL	SB ST ME	0	
	BC	80>90	5YR 3/4	C	SB ST ME	0	
EA007	Ap	0-10	10YR	HC	GR MO FI	2	0
	Bw	10-50	7.5YR	HC	SG MO ME	5	
	BC	50>90	7.5YR	HC	SG ST VC	2	
EA008	Ap	0-10	7.5YR	C	GR ST FI	40	0
	Bw	10>40	5YR	HC	SB MO CO	70	
EA009	Ap	0-10	7.5YR	HC	GR MO FI	30	0
	Ah	10-40	7.5YR	HC	GR MO ME	30	
	Bw	40>50	7.5YR	C	SB ST ME	50	
EA010	Ap	0-10	7.5YR	SL (CP)	GR WE VF	5	0
	Ah	10-30	7.5YR	SL (CR)	SB WE VF	5	
	Bw	30-50	7.5YR	L	SB WE VF	5	
	R	>50	-	-	-	-	
EA011	Ap	0-20	10YR	CL	GR ST ME	30	0
	R	>20	-	-	-	-	
EA012	Ap	0-15	10YR	C	GR MO FI	5	0
	B	15-35	10YR	HC	SB ST ME	5	
	C1	35-80	10YR	HC	SG ST ME	10	
	C2	80>90	10YR	HC	SG ST ME	10	
EA013	Ap	0-10	7.5YR	HC	SB ST FI	10	2
	Bw	10>40	7.5YR	HC	MA ST -	20	
EA014	Ap	0-15	2.5Y	HC	SB MO ME	2	0
	C	15>90	2.5Y	HC	SG ST CO	2	
EA015	Ap	0-15	2.5Y	HC	SB MO FI	5	0
	C	15>90	2.5Y	HC	SG ST CO	5	
EA016	Ap	0-5	7.5YR	CL	GR MO FI	2	0
	Bt1	5-35	7.5YR	SiC	SB ST ME	2	
	Bt2	35>40	7.5YR	SiC	SB ST ME	40	
EA017	Ap	0-15	10YR	SC	GR MO FI	10	0
	Ah?	15>35	2.5Y	SC	SB MO ME	20	
EA018	Ap	0-10	7.5YR	SiL (CP)	GR WE VF	40	0
	Bt	10-30	5YR	SiL (CR)	GR MO FI	40	
	R	>30	-	-	-	-	

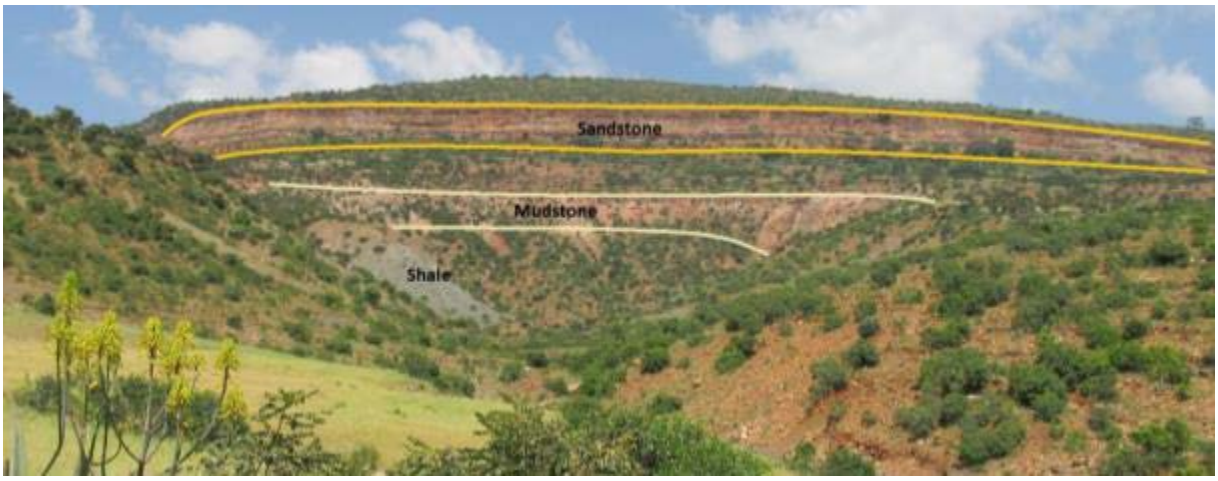

Figure 13: Picture interpretation of different rock types outcropping around a gully on the East slope of the Mymisham Ridge (Paul, 2013).

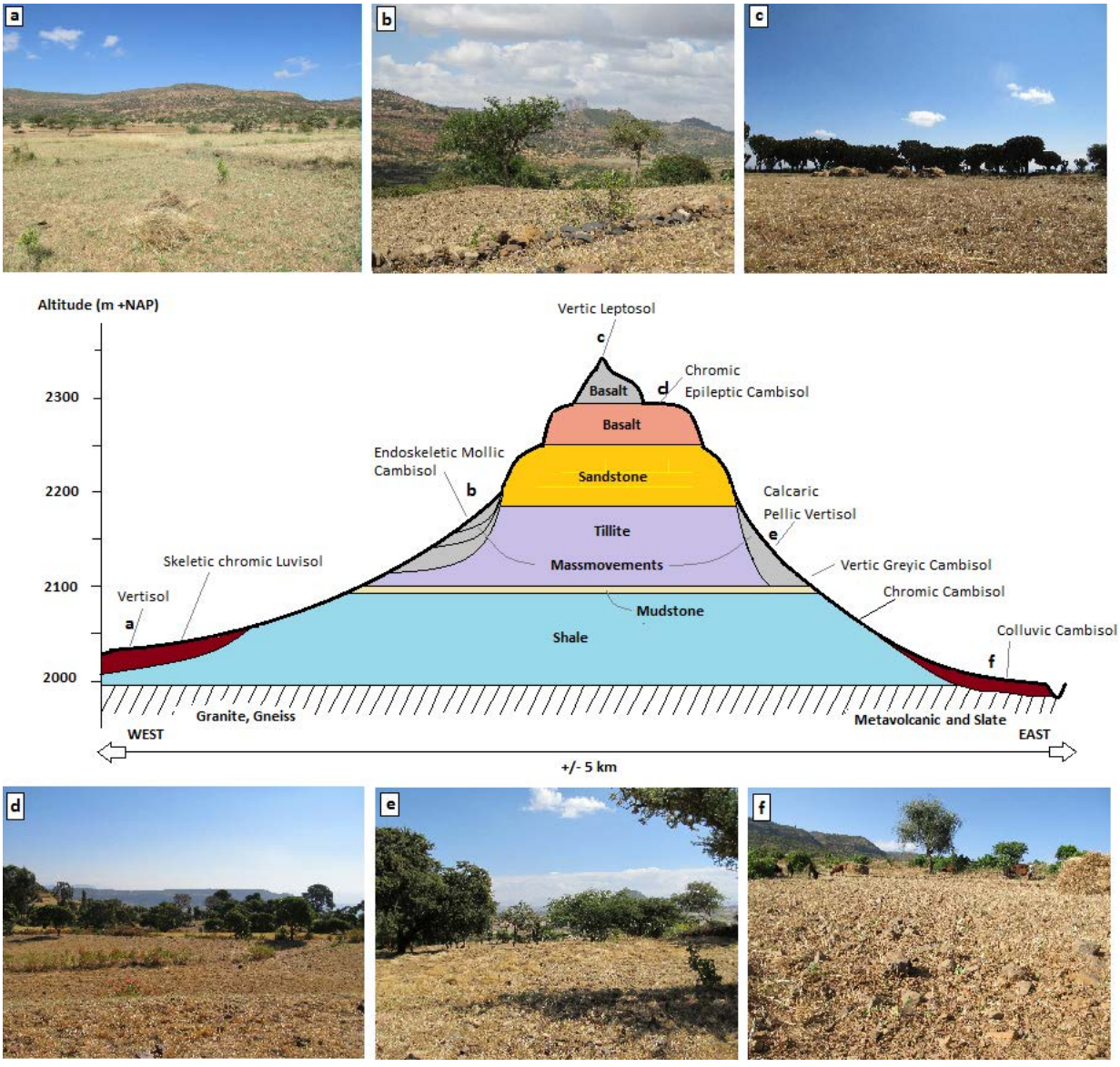

Figure 14: The Mymisham soil catena. The bold letters correspond to the location of the landscape picture with the same letter.

Figure 15: The river Mayira during the rainy season (Kraaijvanger, 2010).

Figure 16: The bluish/grey shale with laminations (Kraaijvanger, 2010).

Figure 17: On the left; The river Mayira cuts through the bedrock of metavolcanic rock. The arrow indicates a vein of quartz. On the right; A pellic Vertisol with big cracks. The boulders on the surface are both basalt and sandstone and possible others (like limestone). The remnants of the crop teff can be seen, one of the few crops that is grown on these heavy soils.

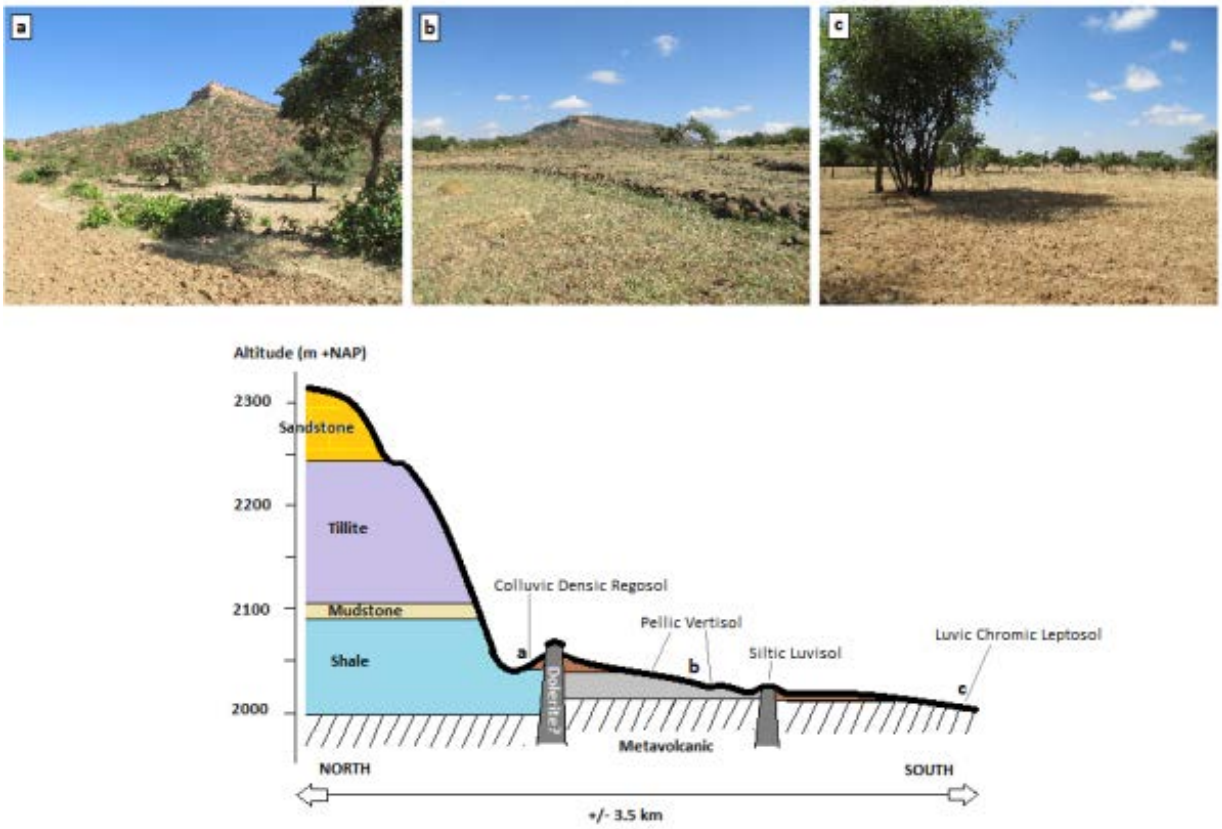

Figure 18: The Zonghi soil catena. The bold letters correspond to the location of the landscape picture with the same letter.

The Zonghi transect starts in the North from the sandstone plateau, but because this was all area exclosure this section was not sampled. On the way to the transect, the typical blue tillite showed at the slopes and the surface. The first measurement point was located at the footslope of a rock outcrop (Figure 18a, Table 2; EA017). This hill clearly stood out and must therefore be of a harder material then the surrounding shales. I suspects it could be a dolerite dyke, but I have not examined

this hypothesis in detail. Moving to the south a relatively flat (it actually has a small but steady gradient) and open area appears (Figure 18b), undesired by the local farmers (but in agricultural use anyway; common crops there are teff and linseed), because of the dark heavy clay soils (Table 2; EA014 & EA015). A prominent feature of this soil are the quartz stones on the surface. I presume this soil is formed from the metavolcanic bedrock with the quartz veins and lays in a stable position between the first dyke and another, preventing it from washing away. On a small local hill a Luvisol, a well-developed/older clay soil, was found (Table 2; EA016). Behind this hill, another plain stretched to the horizon (Figure 18c). Although it looked like a location for a deep soil, it turned out to be shallow (Table 2; EA018). At this point, the pediplain began and we choose to end the transect, because the Mymisham table-mountain was not visible anymore, figuring that its influence on soil development no longer be important.

4.1.3 DATA LAYERS AND TOOLS

With use of the literature knowledge on geology, picture interpretations and own observations, the available auxiliary data was classified into explanatory variables for prediction of the target variables; soil type, texture and organic matter content. The most important step was to derive a geomorphological map from the DEM. The resulting map is displayed in Figure 19. The rules for classification can be seen in the decision tree (Table 3).

When taking the spatial distribution of the geology into account, these layers of rocktypes seem to lay practically horizontally when the structure of the table mountain is concerned. Under this assumption the classification rules can be directly based on the absolute elevation. Table 3 shows the classification tree for geomorphology based on this point. A zone of 25 meters relative altitude is used to indicate the area closest to the river, including the riverbed were gravel is deposited and the colluvial Vertisols, Cambisols and Regosols. When comparing Figure 19 with 20, it shows that the location of steep slopes is indeed the border of geomorphological units, like was hypothesized in the method (Section 3.1.3).

In the Zonghi area South-west of the ridge, it can be seen on the satellite photograph (Figure 6) that there are multiple soil colours. This indicates different parent materials, but it is not neatly layered due to folding and faulting, which made it impossible to distinguish further. With this method of classification it is also hard to distinguish the dykes/sils and the outcropping rock that belongs to it, because they are “accidental” features with only a small size. It is also impossible to set-up a rule based structure for the spatial distribution of individual mass-movements of colluvium down slope. Now I have established a zone of 1.5 km around the table-mountain. This distance is approximately the distance from the sandstone cliff to a point at the river bank of where I know colluvial material lays, so this zone is far from accurate. For the aerial photograph based model of Van de Wauw et al. (2008), these landslides were delineated visually with expert knowledge on features that suggest the presence of them.

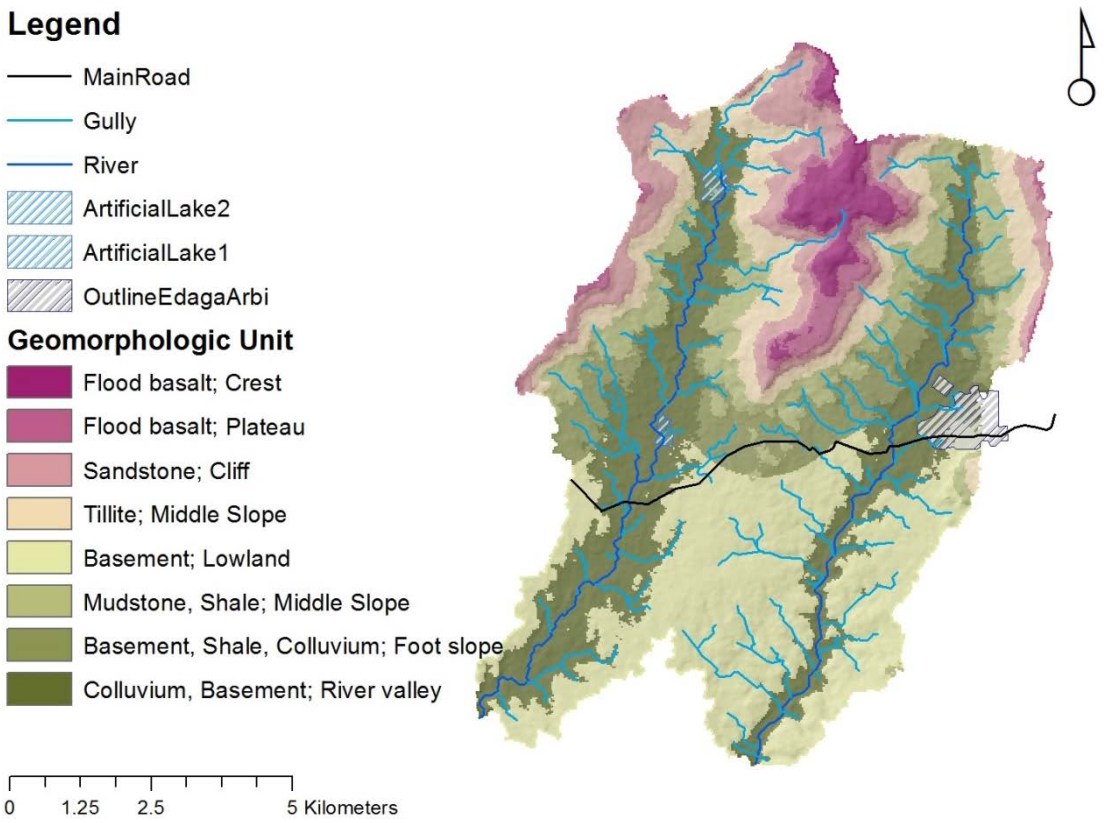

Figure 19: Map of the geomorphology based on absolute and relative elevation and expert knowledge.

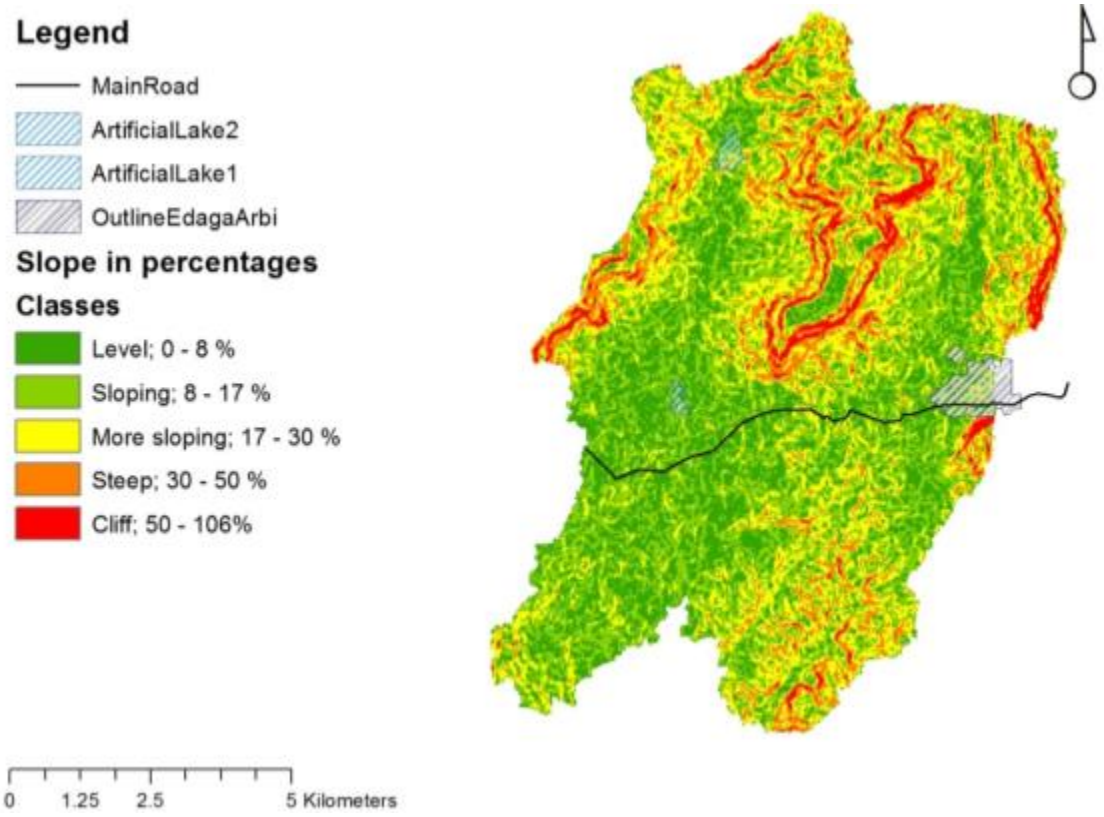

Figure 20: Five categories of slope

Table 3: Decision tree for geomorphology classification

Altitude	Geology	Range of 1.5 km around Sandstone cliff	Geomorphologic unit
abs. >2310	Flood basalt 2		Crest
abs. 2276-2310	Flood basalt 1		Plateau
abs. 2186-2276	Sandstone		Cliff
abs. 2107-2186	Tillite, Colluvium		Middle Slope 1
abs. 2041-2107	Mudstone, Shale, Colluvium		Middle Slope 2
abs. <2041	Basement, Colluvium	Within range	Foot Slope
		Outside range	Low land
rel. < 25	Colluvium		River valley

To demonstrate the small distanced variability in the area, Figure 21 and 22 are included. These show the distribution of concave and convex positions and ridges in the area, which change every 100 meter. These layers can be used in further analysis to indicate stable and unstable positions in the landscape, resulting in different soil development. Ridges are basically the locations of zero flow accumulation and therefor local heights. Being in a top position does not directly mean that it is a convex position too, in some few cases a concave top position exists. The ridges appear to be everywhere, only slightly less profound just below the sandstone cliff on the middle slope. This means that the whole study area is dissected by gullies and subject to soil movement in the form of soil erosion.

In the land-cover map of Figure 23, the most negative NDVI values of -0.28 till -0.13 reflect the artificial lake (the second was not yet build in 2005); values -0.13 – 0.01 are classified as build-up area and landslides; the bare soil class (0.01 – 0.11) follows the river and gully pattern throughout the landscape; arable land covers the range of smallest values with vegetation (0.11 – 0.20), because the image is taken at harvest time (crops turn yellow); the next class (0.20 – 0.24) is arable land with trees planted in and around the fields, the green leaves of the trees give a slightly higher NDVI; The highest range of values (0.24 – 0.42) are classified as semi-natural vegetation of shrubs and young trees.

From the land-cover map (Figure 23) it becomes clear that the Mayira basin is a lot barer than the Seysa basin. This can be explained by the deeper incising Mayira river, the erosion leads to steep unstable slopes and bare rock. This is of course unfortunate for agriculture. In the Seysa basin, south of the main road, in the area that is called Zonghi, the population tried agro-forestry to counter soil erosion and degradation. This is clearly reflected. This type of agriculture could also have an effect on the SOM content of the topsoil. The most condensed vegetation densities can be found on the mountains, it is striking that the table mountain is so well lined. This vegetation is mostly part of area enclosures on the steep slopes.

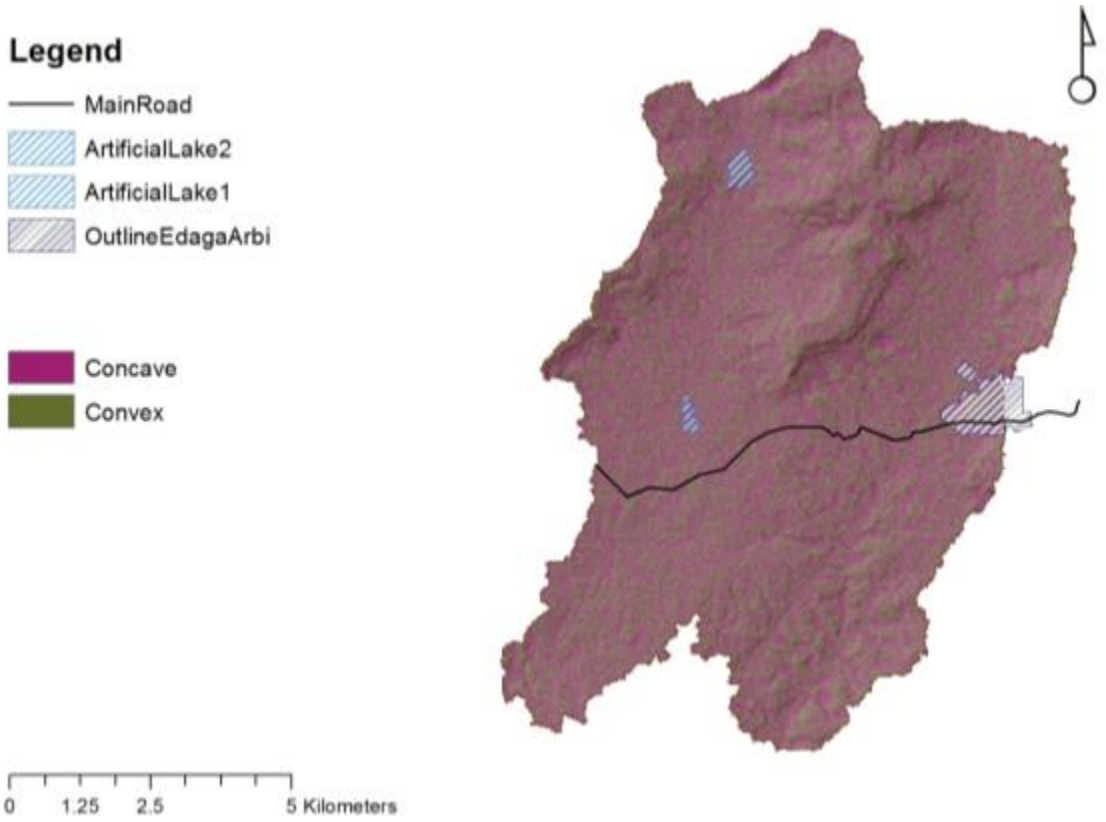

Figure 21: Curvature (second derivative of topography).

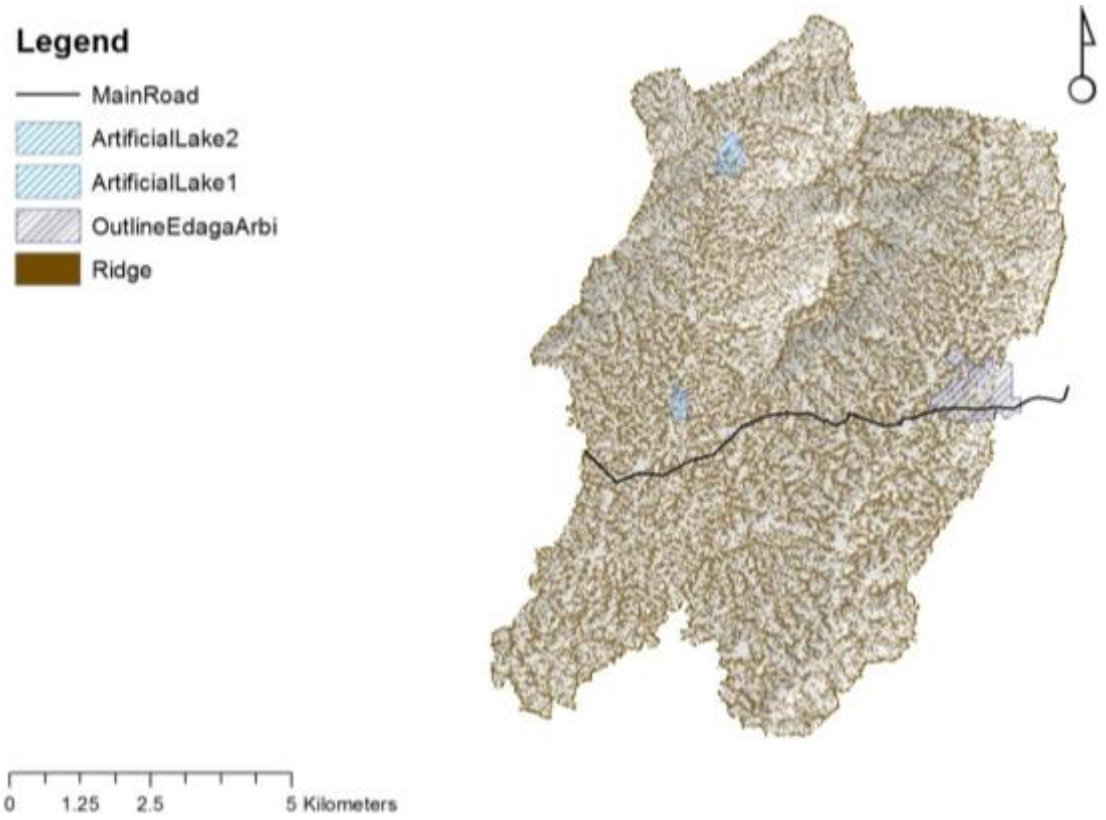

Figure 22: Zero flow accumulation indicates ridges; local hilltops.

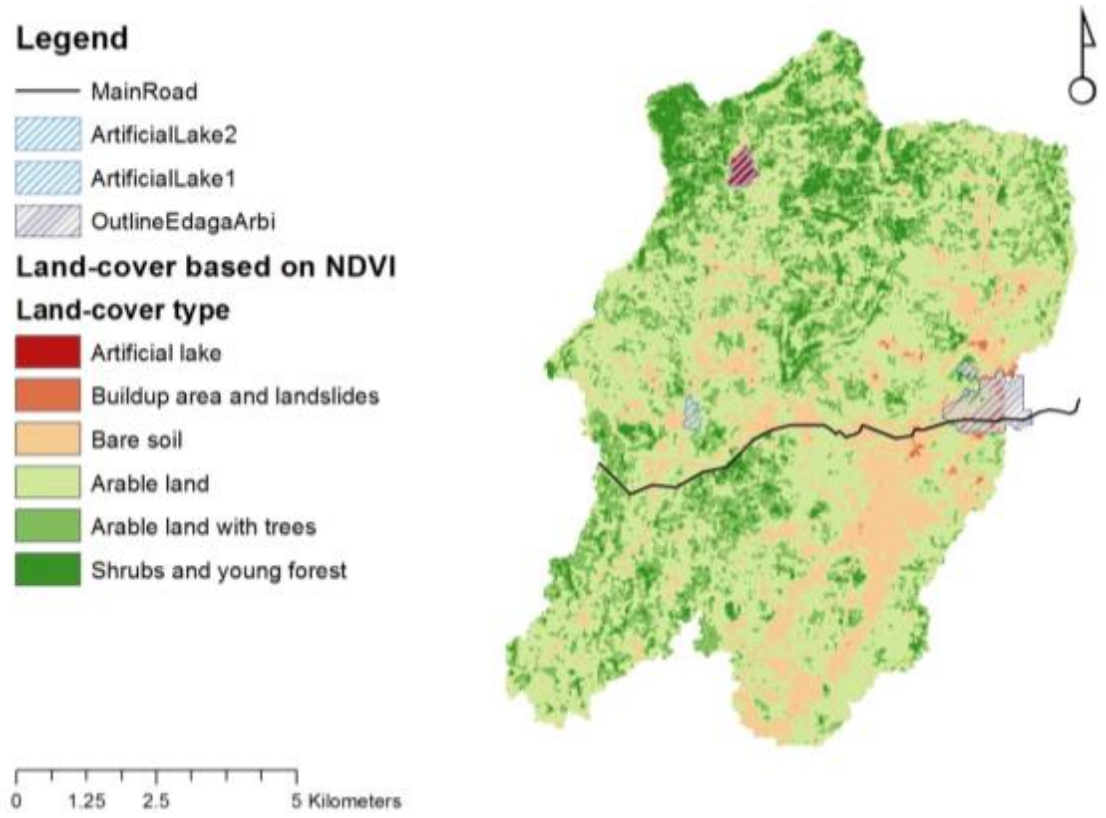

Figure 23: land-cover types based on NDVI (23 Oct. 2005). The land-cover types have NDVI's of respectively: -0.28 - -0.13; -0.13 – 0.01; 0.01 – 0.11; 0.11 – 0.20; 0.20 – 0.24; 0.24 – 0.42.

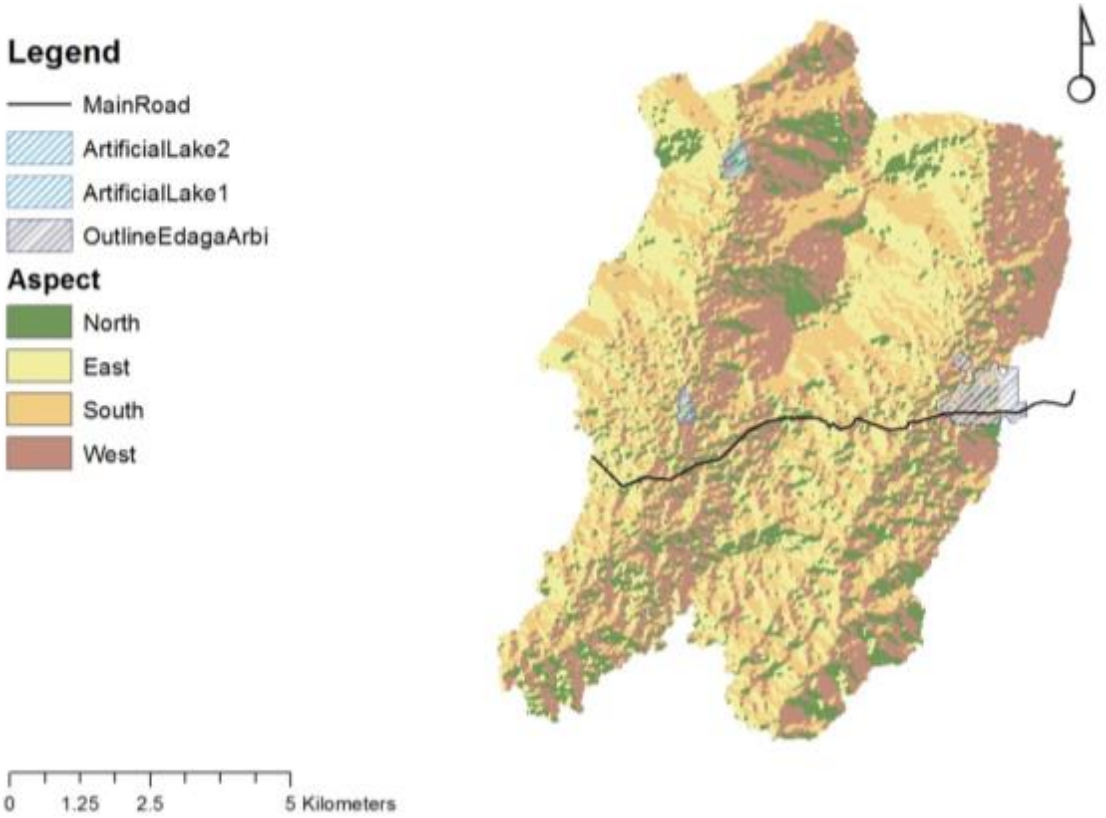

Figure 24: Aspect displaying varying incoming sunlight intensity and therefor differences in soil development due to retention and evaporation of the soil moisture content.

The map of the aspect (Figure 24) can be used to distinguish small differences in micro-climate (this is the last soil forming factor), because the direction a slope is facing account for different amounts of direct sunshine. South facing slopes receive the most sunshine, in contrast to North facing slopes, which lay in the shade most of the time. A south facing slope will become warmer and will lose more moisture due to evapotranspiration, than a North facing slope. This will lead to differences in vegetation cover and soil development.

4.1.4 THE DECISION TREE MODELS

To map the distribution of the different soil properties and types, three different tree-models are made. The first is for soil type (Table 4), the second for texture class (Table 5) and the last for organic matter content (Table 6). The literature and the transect study gave a clear insight in the spatial distribution of the different soil types in the area. Therefor the rules for the decision tree were not hard to indicate. Also the colour variation and stoniness of the soil could be implemented by the use of qualifiers, giving the resulting map another level of detail (Figure 26). However the relationships in order to predict texture and SOM on the level of detail that were preferred, were not that well understood. Much of the gaps in those models are filled based on educated guess.

All decision trees are based on a first classification by geomorphology, because this gives the first important distinguishment for soil development; both parent material and topography. Although it should be noted that this classification is in fact only based on altitude, it correlates with the horizontal layering of the rocktypes. In the case of soil type and texture, the next divide lays with slope. The amount of slope is important as an indication for the erosion sensitivity and the possible age of the soil as a result. The 'flat' and 'lightly sloping' areas (slope of 0-17%) I took together and gave these surfaces another distinction, namely ridges. This because I saw that in this area slight elevation differences in de form of local heights and depressions determined the differences in soil development. Only when the slope is higher than 17%, then the slope is the only important factor next to geomorphology. In summary:

$$S_{type} = f(\text{geomorphology, slope, ridges}) \text{ and } S_{texture} = f(\text{geomorpology, slope, ridges})$$

The decision tree for SOM is based on geomorphologic units put together, without the distinction of slope. I decided this way to roughly distinguish between of estimated age of the soil giving one soil more time to develop a higher SOM content then the others. The second classification step is aspect for the micro-climate reasons. At last the vegetation type influences the amount of dead organic matter that can recede to SOM. This way, the SOM content in the soil it is more or less in equilibrium with the input and decomposition. Although this environment is far from a natural one, it is in fact an ancient agricultural area, there were no clear patterns to implement it otherwise. The predicted values in Table 6 are estimations based on the distribution (mean and standard deviation) of Table 1. The following model was the result:

$$S_{SOM} = f(\text{geomorphology, aspect, land-cover type})$$

Table 4: Decision tree for soil type

Geomorphology unit	Slope	Ridge	Qualifier(s) Soiltype
Crest	Flat and lightly sloping	Yes	Vertic Leptosol
		No	Pellic Vertisol
	More sloping		Vertic Cambisol
	Steep		Chromic Leptosol
	Cliff		Bare Rock
Plateau	Flat and lightly sloping	Yes	Chromic Cambisol
		No	Chromic Luvisol
	More sloping		Epileptic Cambisol
	Steep		Chromic Leptosol
	Cliff		Rare Rock
Cliff area	Flat and lightly sloping	Yes	Chromic Leptosol
		No	Skeletic Regosol
	More sloping		Epileptic Cambisol
	Steep		Leptosol
	Cliff		Bare Rock
Middle Slope 1	Flat and lightly sloping	Yes	Vertic Cambisol
		No	Pellic Vertisol
	More sloping		Skeletic Cambisol
	Steep		Leptosol
	Cliff		Bare Rock
Middle Slope 2	Flat and lightly sloping	Yes	Chromic Cambisol
		No	Vertic Cambisol
	More sloping		Epileptic Cambisol
	Steep		Chromic Leptosol
	Cliff		Saprolite
Foot Slope	Flat and lightly sloping	Yes	Chromic Regosol
		No	Skeletic Regosol
	More sloping		Epileptic Regosol
	Steep		Leptosol
	Cliff		Saprolite
Low Land	Flat and lightly sloping	Yes	Chromic Luvisol
		No	Pellic Vertisol
	More sloping		Epileptic Chromic Luvisol
	Steep		Luvic Chromic Leptosol
	Cliff		Bare Rock
River valley	Flat and lightly sloping	Yes	Vertic Cambisol
		No	Vertisol
	More sloping		Skeletic Regosol
	Steep		Leptosol
	Cliff		River, gully incision

Table 5: Decision tree for texture in the top- and subsoil.

Geomorphology unit	Slope	Ridge	Texture class: topsoil (10cm), subsoil (40cm)
Crest	Flat and lightly sloping	Yes	Heavy clay, rock
		No	Heavy clay, heavy clay
	More sloping		Clay, clay
	Steep		Clay, rock
	Cliff		Bare Rock, rock
Plateau	Flat and lightly sloping	Yes	Loamy sand, sandy loam
		No	Clay loam, clay
	More sloping		Sandy loam, clay loam
	Steep		Sandy loam, rock
	Cliff		Bare Rock, rock
Cliff area	Flat and lightly sloping	Yes	Loamy sand, rock
		No	Sandy loam, Sandy loam
	More sloping		Sand, Sandy loam
	Steep		Sand, rock
	Cliff		Bare Rock, rock
Middle Slope 1	Flat and lightly sloping	Yes	Clay, heavy clay
		No	Heavy clay, heavy clay
	More sloping		Clay, heavy clay
	Steep		Clay loam, rock
	Cliff		Bare Rock, rock
Middle Slope 2	Flat and lightly sloping	Yes	Sandy clay, clay
		No	Sandy clay, sandy clay
	More sloping		Sandy clay, clay
	Steep		Sandy clay, saprolite
	Cliff		Saprolite, rock
Foot Slope	Flat and lightly sloping	Yes	Sandy clay, clay
		No	Clay, heavy clay
	More sloping		Sandy clay, Sandy clay
	Steep		Sandy loam, saprolite
	Cliff		Saprolite, rock
Low Land	Flat and lightly sloping	Yes	Clay loam, silty clay
		No	Heavy clay, heavy clay
	More sloping		Clay loam, silty clay
	Steep		Clay loam, rock
	Cliff		Bare Rock, rock
River valley	Flat and lightly sloping	Yes	Heavy clay, heavy clay
		No	Silty clay, silty clay
	More sloping		Clay loam, clay
	Steep		Clay loam, rock
	Cliff		River, gully incision

Table 6: Decision tree for SOM

geomorphologic unit	Aspect	Land-cover	Soil Organic Matter (SOM)
Crest, Plateau	West, North	Bare soil	3.5
		Arable lands	3.8
		Arable lands with trees	4.1
		Semi-natural vegetation	4.4
	East, South	Bare soil	2.5
		Arable lands	2.8
		Arable lands with trees	3.1
		Semi-natural vegetation	3.4
Middle Slope, Lowlands	West, North	Bare soil	2.5
		Arable lands	2.8
		Arable lands with trees	3.1
		Semi-natural vegetation	3.4
	East, South	Bare soil	1.5
		Arable lands	1.8
		Arable lands with trees	2.1
		Semi-natural vegetation	2.4
River valley, Foot slope, Sandstone cliff area	West, North	Bare soil	1.5
		Arable lands	1.8
		Arable lands with trees	2.1
		Semi-natural vegetation	2.4
	East, South	Bare soil	0.5
		Arable lands	0.8
		Arable lands with trees	1.1
		Semi-natural vegetation	1.4

4.2 MODEL VALIDATION

Within this section the model will be validated by testing the accuracy of the maps (Section 4.2.2), but first, the structure of the decision tree will be analysed by examining the fraction of explained variability of each explanatory variable (Section 4.2.1).

4.2.1 ANALYSIS OF THE DECISION TREE

The results of the ANOVA are displayed in Table 7 and 8. When comparing Table 7 with Table 1, both the validation and the transects datasets show the same spatial variation (almost the same distribution around a similar mean); they are not significantly different. This information can be used as a first indication of the accuracy of the model prediction, as we can say that de data that has served as input to the model is indeed representative for the rest of the area.

Table 7: Mean and standard deviations of various soil properties from the validation sample points in the Edaga Arbi study area.

Soil Property	Surface Stoniness	Munsell Value	Munsell Chroma	Munsell SOM	pH	Nitrogen	SOM from N	Clay Top	Clay Sub
Unit	%	-	-	%	-	%	%	%	%
Mean	58	3.1	3.1	2.2	7.3	0.091	1.9	33-51	43-62
SD	21	0.43	1.1	1.3	0.20	0.046	0.9	23	18

Table 8: Fraction (in %) of explained variability of various classifications, significance on p < 0.05 level is indicated with a (*). The '+' means this classification is first based on geomorphology and then secondly the layer mentioned.

	Soil Property	Surface Stoniness	Munsell Value	Munsell Chroma	Munsell SOM	pH	Nitrogen	SOM from N	Clay Top
classification	Geo-morphology	17	40*	38*	54*	33	8	8	21
	+ Slope	38	55	55	69	49	36	36	49
	+ Land-cover	25	47	58	63*	56	36	36	44
	+ Aspect	51	69	69	72	61	40	40	51
	+ Curvature	36	49	54	62*	41	26	26	45
	+ Ridges	38	61	44	60*	46	26	26	43
	Land-cover	7	36*	12	13	8	7	7	6

In Table 8, I noted the outcome of explained variance per different classification. The first is based on the geomorphology only. These eight classes mainly explain the variability of soil colour (value: 40%, chroma: 38% and SOM derived from colour 54%) and not so much the fertility properties (nitrogen and SOM derived from the N content both only 8% - this is a linear relationship (Section 3.1.2.2) explaining the similarity). The variability in surface stoniness, pH and clay fraction in the topsoil is intermediately explained by the geomorphology classification with respectively 17, 33 and 21%. The significance in explaining the soil colour is of course logical, because different colour is a reflection of different parent material plus organic matter and that is exactly what this classification is based on, together with relief. The variability that is experienced (Table 7) with the other soil properties will maybe be explained by another soil forming factor, e.g organisms: land-cover or land-use. Information on land-cover was available through NDVI (while auxilliary information on the other soil forming factors is not available), so this was tested. The fractions of explained variance for the land-cover classification were low (approximately 10%) for most soil properties, except soil colour value (36%). Actual land-cover does not directly influence soil development in this case.

With the other layers which are derivatives of the ASTER DEM, but also the NDVI, I then tried to refine the classification and increase the explained variance. Overall the fraction of explained variance increases, however the significance decreases. This is due to the increasing number of groups in relation to the total sample size which stays 32 (many groups only have one, or even none, sample point representing them).

In the classification tree, a choice was made to use 'ridges' over 'curvature'. It does not really matter to use the one over the other, because it has similar explained variance of which only the variability in Munsell SOM is significantly explained (Table 8).

4.2.2 MAP ACCURACY

In this section the accuracy of the modelling results for major soil type, texture class and organic matter content will be examined and discussed.

4.2.2.1 SOIL TYPE

The outcome of the soil-type tree model can be seen in the map of Figure 23 and the accuracy assessment in Table 9.

From Figure 23 one could clearly distinguish the geomorphologic units. Secondly is the pattern that soil types follow the slope and at last in the 'flattest' areas (slope smaller that 17%) the local heights 'pop out' with in general a more developed, older, brighter colour and/or shallower soil. This results in pellic Vertisols and vertic Leptosols on the basalt flow, chromic Cambisols and Luvisols on the plateau, (pellic) Vertisols and vertic Cambisols below the sandstone cliff (the cliff is in grey), followed by Cambisols and Regosols in the downward direction. Close to the river (relative elevation up to 25 m zone) Vertisols and vertic Cambisols exsist. In the Zonghi area, below the main road, the Vertisols are alternated by Luvisols on the local heights. These soil types are of course how they were modelled (Table 4).

Table 9: Confusion matrix for soil type.

		Ground truth					No. classified points	Users accuracy
		Luvisol	Vertisol	Cambisol	Regosol	Leptosol		
Classified	Luvisol	**2**	1	0	0	4	7	0.29
	Vertisol	1	**4**	2	1	0	8	0.50
	Cambisol	1	1	**4**	0	1	7	0.57
	Regosol	1	1	1	**4**	0	7	0.57
	Leptosol	0	0	1	0	**2**	3	0.67
No. ground-truth points		5	7	8	5	7	**32**	
Producers accuracy		0.40	0.57	0.50	0.8	0.29		**0.50**

The accuracy assessment was done for the main soil type level, because the distinction of qualifiers would require more validation points. Overall the classification of the main soil types has a total accuracy of 50%. This is exactly on the threshold of commonly accepted accuracies. Taghizadeh-Mehrjardi et al. (2014) applied decision tree analysis with use of a digital elevation model, Landsat imagery and a geomorphologic map to predict the spatial location of soil classes in Great Group level for an arid region in Iran. They acquired an overall accuracy of 67.5%, of which they say is similar to the results obtained by other researchers (e.g. Moran and Bui, 2002; Bui et al., 1999; Henderson et al., 2005; Luoto and Hjort, 2005; Jafari et al., 2012). This means that the accuracy of 50% is less than usual with use of the same approach and similar study area (climate and accessibility).

The users accuracy is for most classes (Vertisols, Cambisols, Regosols and Leptosols) even higher (in de range of 50 to 67%) , but the classification of Luvisols has gone wrong with an users accuracy of 29%; what was classified as one was in fact a Leptosol in most cases (4 out of 7 cases). This is also reflected in the producers accuracy of the Leptosols, which is only 29% in relation with the other classes with accuracies ranging from 40 to 80%.

I studied the possibility to change the classification in such a way that some classified Luvisols will classify as Leptosols in an improved version of the model as illustrated in Figure 25. This improvement needs further testing first, which requires calibration points that are not available.

Foot Slope	Flat and lightly sloping	Yes	Chromic Regosol
		No	Skeletic Regosol
	More sloping		Epileptic Regosol
	Steep		Leptosol
	Cliff		Saprolite
Low Land	Flat and lightly sloping	Yes	*Epileptic chromic Luvisol*
		No	Pellic Vertisol
	More sloping		*Luvic Chromic leptosol*
	Steep		*Chromic Leptosol*
	Cliff		Bare Rock
River valley	Flat and lightly sloping	Yes	Vertic Cambisol
		No	Vertisol
	More sloping		Skeletic Regosol
	Steep		Leptosol
	Cliff		River, gully incision

Figure 25: Part of the improved tree model, the changed entries are indicated in *italic.* the remainder of the model stays the same. It should be noted that this is a proposal which is not yet tested.

It could be that I am overestimating the amount of surface that is in fact a Luvisol, but considering my own observations and that of colleagues in similar areas, it could also be that those Leptosols are the outliers. The observations show these soils are classified as Leptosols due to a high gravel and rock content leading to a very dense layer which was hard to go through. “Pure” Leptosols are only found at specific spots like cliffs and outcrops.

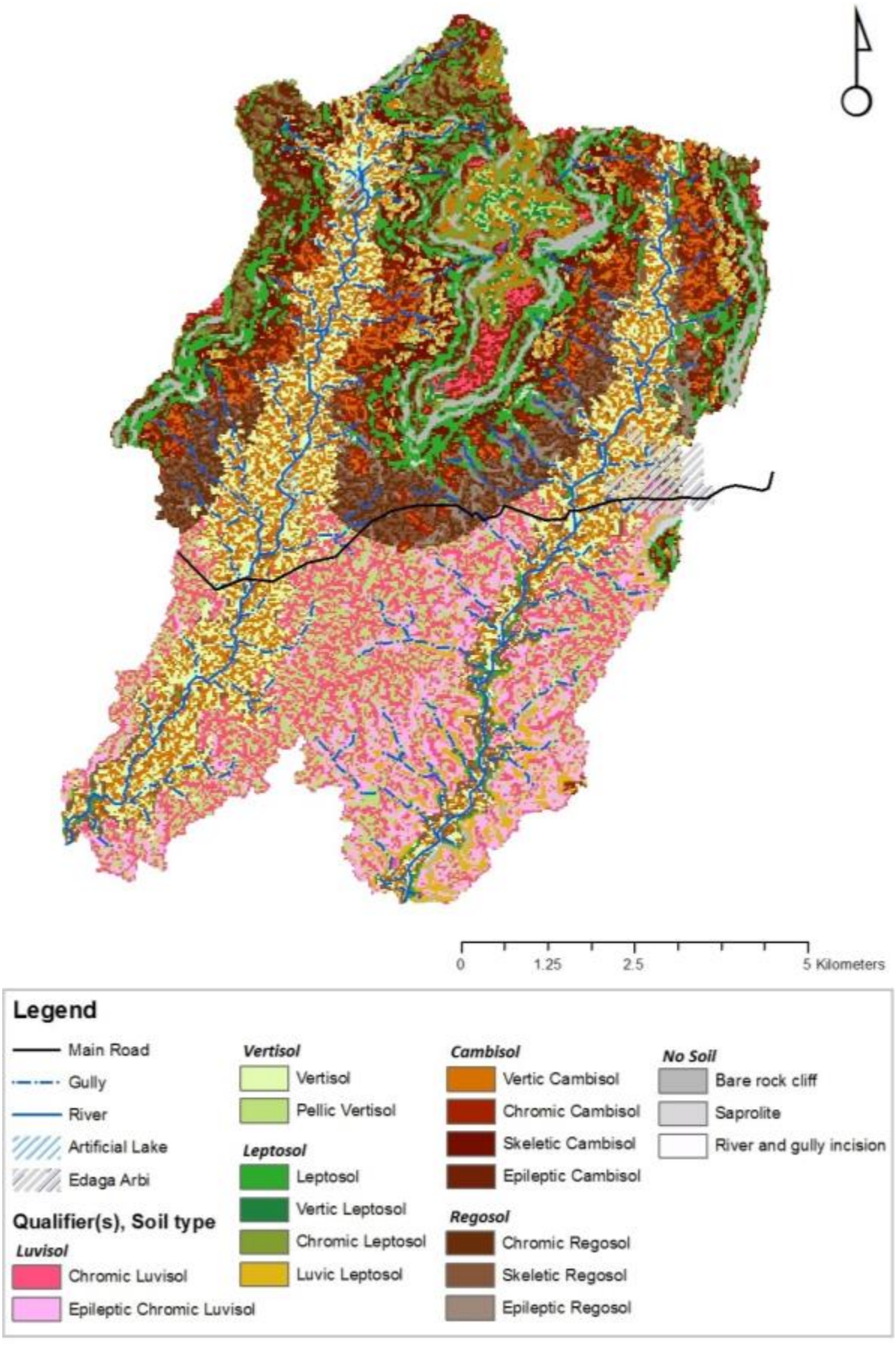

Figure 26: Map of soil types in the Edaga Arbi area around the Mymisham table-mountain.

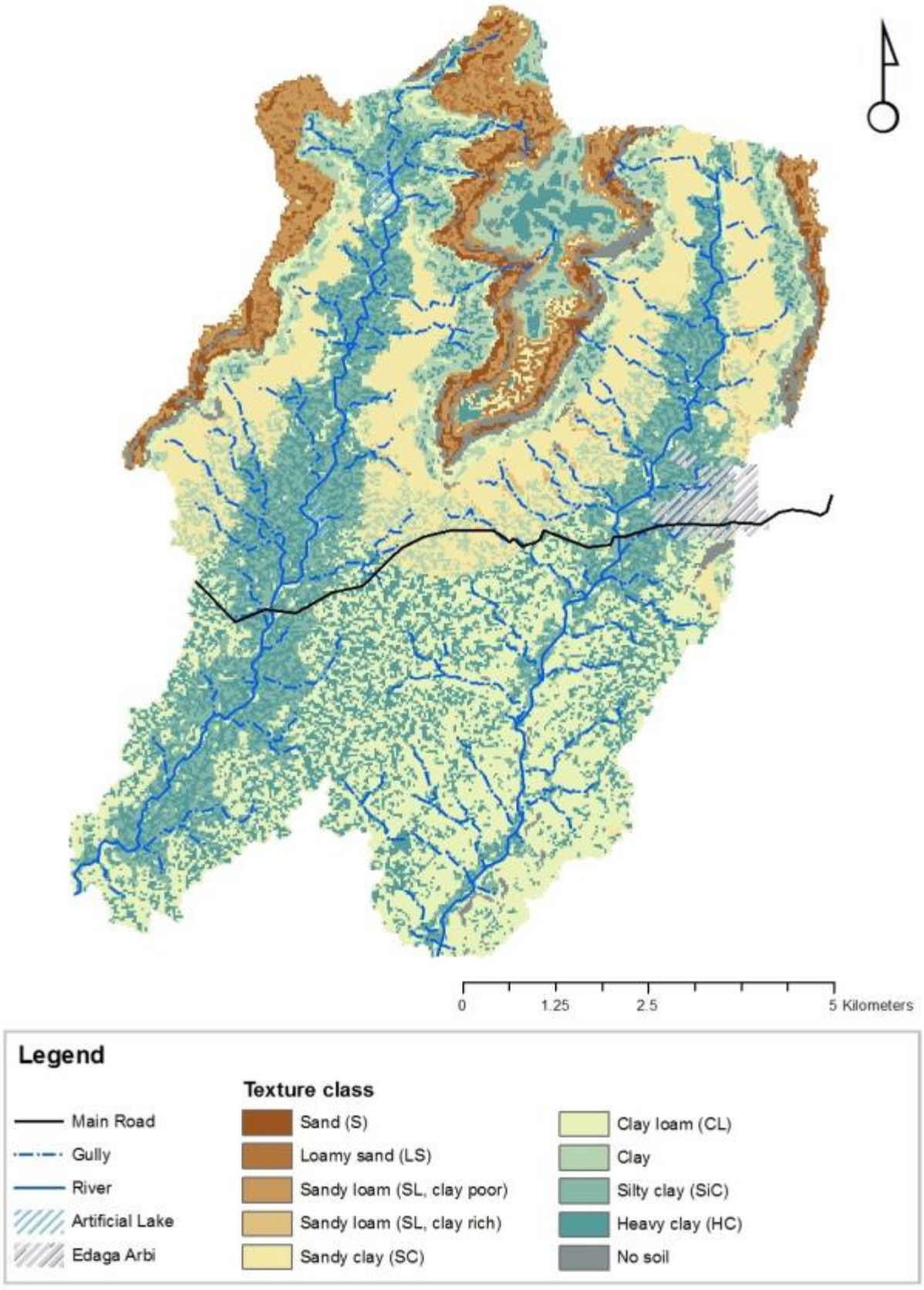

Figure 27: Map of soil texture types.

4.2.2.2 TEXTURE

Figure 27 shows the modelling result for soil texture. This map also highlights the geomorphologic units, slopes and ridges but in a more smooth way. There are mostly different mixes of clay in a pattern that begins with heavy clay on top of the basalt flow and ends with heavy clay in de valley positions. The plateau and its slopes have a more coarse texture. But below the cliff we find the heavy and silty clays again. Below this mixed clay and sand can be found.

Table 10: Confusion matrix for soil texture with texture classes according to table 25 of the guideline to soil description (FAO 2006).

		Ground truth										No. classified points	Users accuracy
		S	LS	SL(p)	SL(r)	SC	CL	C	SiC	HC	LCS		
Classified	S	**0**	0	0	0	0	0	0	0	0	0	0	-
	LS	0	**1**	0	0	0	0	0	0	0	0	1	1
	SL(p)	0	0	**0**	0	0	0	0	0	0	0	0	-
	SL(r)	0	0	0	**0**	0	0	0	0	0	0	0	-
	SC	0	0	0	1	**2**	1	0	1	2	0	7	0.29
	CL	0	0	1	1	1	**4**	1	1	2	1	12	0.33
	C	0	0	0	0	0	0	**0**	0	0	0	0	-
	SiC	0	1	0	0	0	1	0	**1**	0	0	3	0.33
	HC	0	0	0	0	1	3	1	0	**4**	0	9	0.44
	LCS	0	0	0	0	0	0	0	0	0	**0**	0	-
No. ground-truth points		0	2	1	2	4	9	2	2	8	1	**32**	
Producers accuracy		-	0.50	0	0	0.50	0.44	0	0.50	0.50	0		**0.38**

Table 10 holds the accuracy assessment. The users accuracy is low or missing for half of the texture classes. The producers accuracy is mostly made up out of 1 or 0 correct out of 2, resulting in an accuracy of 0 or 50%. Clearly not enough validation points are available to test the variability in soil texture on this level of detail. The total accuracy is only 38%. Therefor another matrix is made in which only the differences between the textures sand, loam and clay are indicated (Table 11).

Table 11: Confusion matrix for soil texture with only the main texture types 'sand', 'loam' and 'clay'. Classification is based on the separations in table 25 of the guideline to soil description (FAO 2006).

		Ground truth			No. classified points	Users accuracy
		Sand	Loam	Clay		
Classified	Sand	1	0	0	1	1
	Loam	0	0	0	0	-
	Clay	1	2	28	31	0.90
No ground truth points		2	2	28	32	
Producers accuracy		0.50	0	1		0.91

The high total accuracy of 91% is of course expected, because the main soil texture is in fact clay in many different mixtures. With this classification the variation that is seen in the field is not sufficiently explained because all will be classified as 'clay'. This result will be very accurate, but does not show the desired detail.

4.2.2.3 SOM

Figure 28 shows the resulting SOM map. Again it highlights the Mymisham table-mountain, this time with the highest values of SOM. The differences between the different geomorphological units are based on the texture and relative age, with finer textures having the capacity to contain more and the increasing age for more build-up of organic matter. The north facing slopes were estimated to have a slightly higher content. In the last stage the vegetation intensity plays a role.

Table 12: Confusion matrix for SOM derived from the nitrate measurement.

		Ground truth								No. classified points	Users accuracy
		0-0.5	0.5-1.1	1.1-1.8	1.8-2.1	2.1-2.5	2.5-3.1	3.1-3.8	3.8-4.4		
Classified	0-0.5	**0**	0	0	0	0	0	0	0	0	-
	0.5-1.1	0	**2**	0	2	0	0	0	1	5	0.40
	1.1-1.8	0	0	**2**	0	0	0	0	0	2	1
	1.8-2.1	0	1	2	**2**	2	0	1	0	7	0.29
	2.1-2.5	0	1	3	1	**2**	0	0	2	9	0.22
	2.5-3.1	0	1	0	2	0	**0**	0	0	3	0
	3.1-3.8	0	2	1	0	2	0	**1**	0	6	0.17
	3.8-4.4	0	0	0	0	0	0	0	**0**	0	-
No. ground-truth points		0	7	8	7	6	0	2	3	**32**	
Producers accuracy		-	0.29	0.25	0.29	0.33	**-**	0.50	0		**0.28**

Table 13: Confusion matrix for SOM derived from the Munsell Soil Colour observation.

		Ground truth								No. classified points	Users accuracy
		0-0.5	0.5-1.1	1.1-1.8	1.8-2.1	2.1-2.5	2.5-3.1	3.1-3.8	3.8-higher		
Classified	0-0.5	**0**	0	0	0	0	0	0	0	0	-
	0.5-1.1	0	**2**	1	0	0	2	0	0	5	0.40
	1.1-1.8	0	2	**0**	0	0	0	0	0	2	0
	1.8-2.1	1	3	0	**0**	0	3	0	0	7	0
	2.1-2.5	0	1	4	0	**0**	4	0	0	9	0
	2.5-3.1	0	1	0	0	0	**1**	0	1	3	0.33
	3.1-3.8	0	0	1	0	0	0	**3**	2	6	0.50
	3.8-4.4	0	0	0	0	0	0	0	**0**	0	-
No. ground-truth points		1	9	6	0	0	10	3	3	**32**	
Producers accuracy		0	0.22	0	-	-	0.10	1	0		**0.19**

Table 12 shows the lowest overall accuracy so far; 28%. Both the users accuracy and the producers accuracy are not sufficient for most of the classes. This could be due to two things: First the understanding of the spatial distribution of this soil property in this area is very limited; the literature was mostly focussed on soil types and the transect data did not provide an overall relationship leaving me with the implementation of the model based on educated guess. This is being reflected in Table 8, the variability was not very well explained by the geomorphology or any other explanatory variable. Second, this limited understanding could be caused by the SOM measurement being

inaccurate, because it is based on the field measurement of nitrate, from which we assume a linear relationship with SOM, which in turn is not calibrated with laboratory measurements. This means that the 'ground truth' values making up the table could differ from the 'real truth' and then also the modelled content. To test these arguments we could also use the SOM values derived from the Munsell soil colour observations. But, like the previous measurements of SOM, these values are also not calibrated and therefor there is no insight into the truth of these observations. The SOM values are estimated based on the assumption that the soil colour is a mixture of dark organic carbon and lighter soil minerals. However, the basalt found in our study area has very dark coloured minerals, making it hard to distinguish with the organic matter content. The confusion matrix can be found in Table 13. It indeed shows that the total map accuracy is even less (19%) with use of the Munsell soil colour observations as validation, than with the nitrate transfer function.

There is one thing that could improve the accuracy, and that is by decreasing the amount of classes, and thereby increasing the range. As the confusion matrixes show (Table 14 and 15), the total accuracies improve but still do not reach the desired level of accuracy, because the ground truth values still fall outside the modelled range. Another explanation emerges and that is that the rule structure in the decision tree model is not correctly defined. Instead of using the aspect on the second level, it is maybe better to use the land-cover. Also the values defined to each geomorphological unit needs looking after. To test this, more observations are needed to form an additional calibration dataset.

Table 14: Confusion matrix for SOM (nitrate derived) with less categories.

		Ground truth				No. classified points	Users accuracy
		0.5-1.5	1.5-2.5	2.5-3.5	3.5-4.5		
Classified	0.5-1.5	**3**	2	0	1	6	0.50
	1.5-2.5	4	**10**	0	3	17	0.59
	2.5-3.5	4	4	**1**	0	9	0.11
	3.5-4.5	0	0	0	**0**	0	-
No. ground truth points		11	16	1	4	**32**	
Producers accuracy		0.27	0.63	1	0		**0.44**

Table 15: Confusion matrix for SOM (Munsell Soil Colour derived) with less categories.

		Ground truth				No. classified points	Users accuracy
		0-1.5	1.5-2.5	2.5-3.5	3.5-higher		
Classified	0-1.5	**3**	1	2	0	6	0.50
	1.5-2.5	6	**4**	7	0	17	0.24
	2.5-3.5	1	1	**4**	3	9	0.44
	3.5-higher	0	0	0	**0**	0	-
No. ground truth points		11	5	13	3	**32**	
Producers accuracy		0.27	0.63	1	0		**0.34**

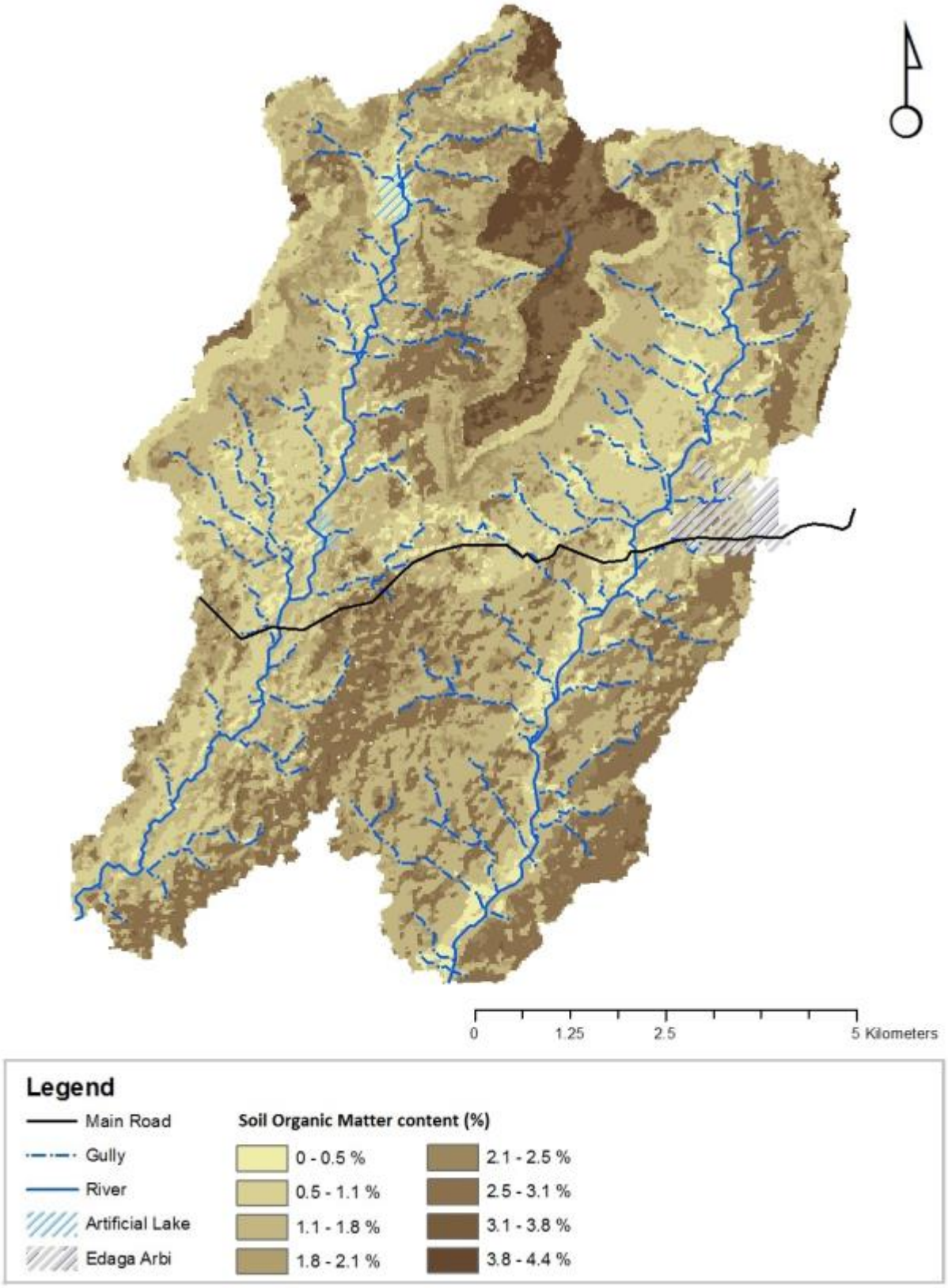

Figure 28: Map of SOM

4.3 MODEL EXTRAPOLATION

In this chapter the extrapolation of the model will be examined. The validation from the previous section did not show a sufficient accuracy for the predictions of texture and SOM, therefor only the model for soil type will be extrapolated. This will proceed according to the following steps: First the similarities and differences between the Edaga Arbi modelling area and the extrapolation area (or extrapolation sites) will be analysed. The main question that is answered in this section is: Are there possible modifications to the auxiliary information layers that need to be taken, in order to have valid assumptions to the model? From this analysis we will select the representable extrapolation sites to test, with use of the extrapolation data, the decision tree model's accuracy for these situations. When the validation is successful, the model can be used to predict the entire regional area, providing they have similar landscape features.

4.3.1 AREA REPRESENTABILITY

The result of the area representability analysis is shown as the extent of the geology map that is displayed in Figure 29a. The extent of the map is defined by a square around one table-mountain complex. As can be seen, both the Edaga Arbi and Inticho region are included in this extent. Hagere Salam and Hawsen are not as they were not similar under the assumptions of horizontal layering and homogeneity of the lithology (Section 3.3.2).

The modelled geologic features are strikingly similar to the drawn geological map in Figure 3. The layer that was first classified as the 'tillite' (middle slope) in the Edaga Arbi region was in fact covered by vertic clays and possible other colluvial material originating from above (4.1.2). For this reason the name of this class has changed in this geology map. The 'freckled' area in the North-west of the map is actually not part of the stepped table-mountain landscape with flood basalts, because it shows in fact weathered volcano centres that sit in the landscape as plugs (steep-sided conical hills), as Hagos et al. (2010) describe. One should not choose to extrapolate the model there, because it will not be representative. With the geology checked, the geomorphology map can also be made, of which the result can be seen in Figure 29b. One difference with the implementation of this regional geomorphology map in contrast to the local EA implementation is that the sandstone 'zone' which was differentiated at first, is now together with the 'plateau' unit. This was done because there was not really a reason in keeping it separate as it is defined automatically by the secondary branching sequence 'slope: cliff'. Together with the colluvial zone around the table-mountain complex this gives seven classes instead of the previous eight.

Since the borders of the representable area are established and the auxilliary information layers prepared, the performance of the soil type model can be examined in detail through an application in the Inticho area. Two of the explanatory data layers, geomorphology and slope are displayed in the extent of the two basins around Inticho in Figure 30.

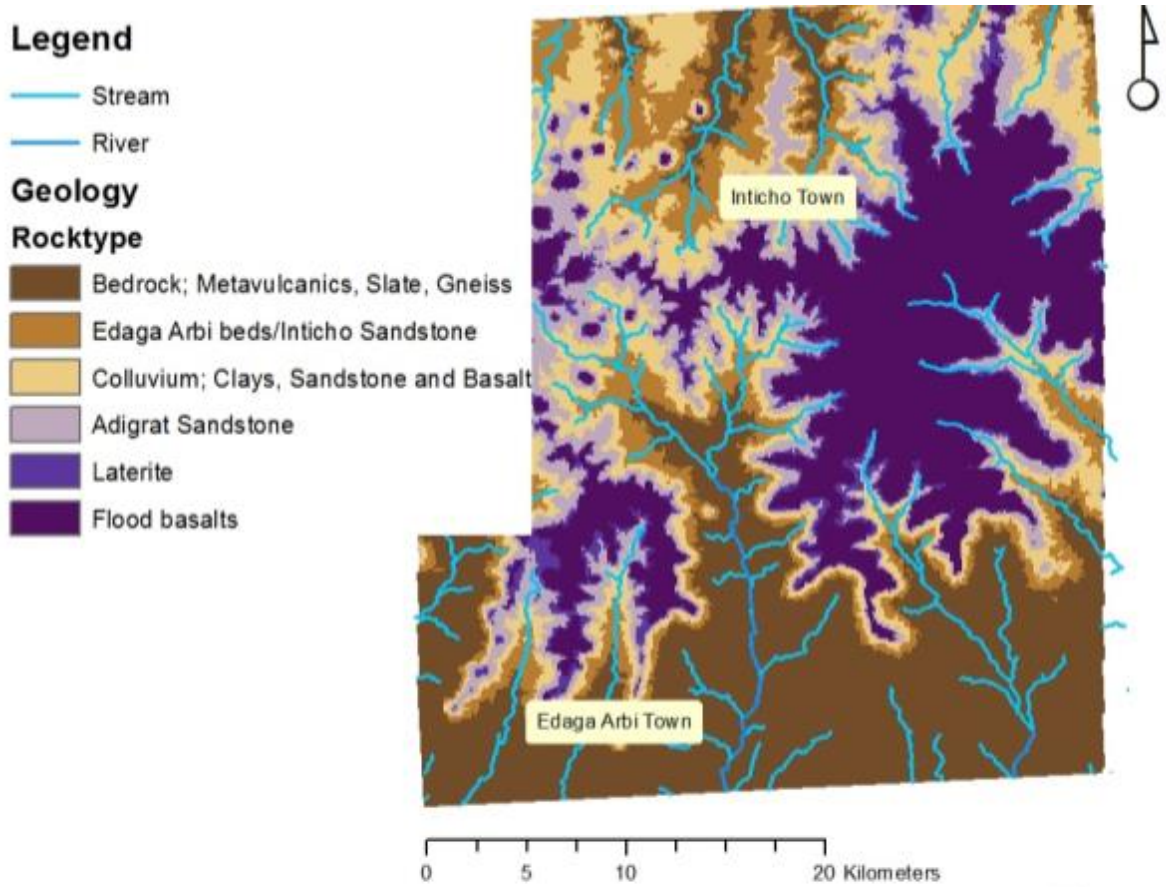

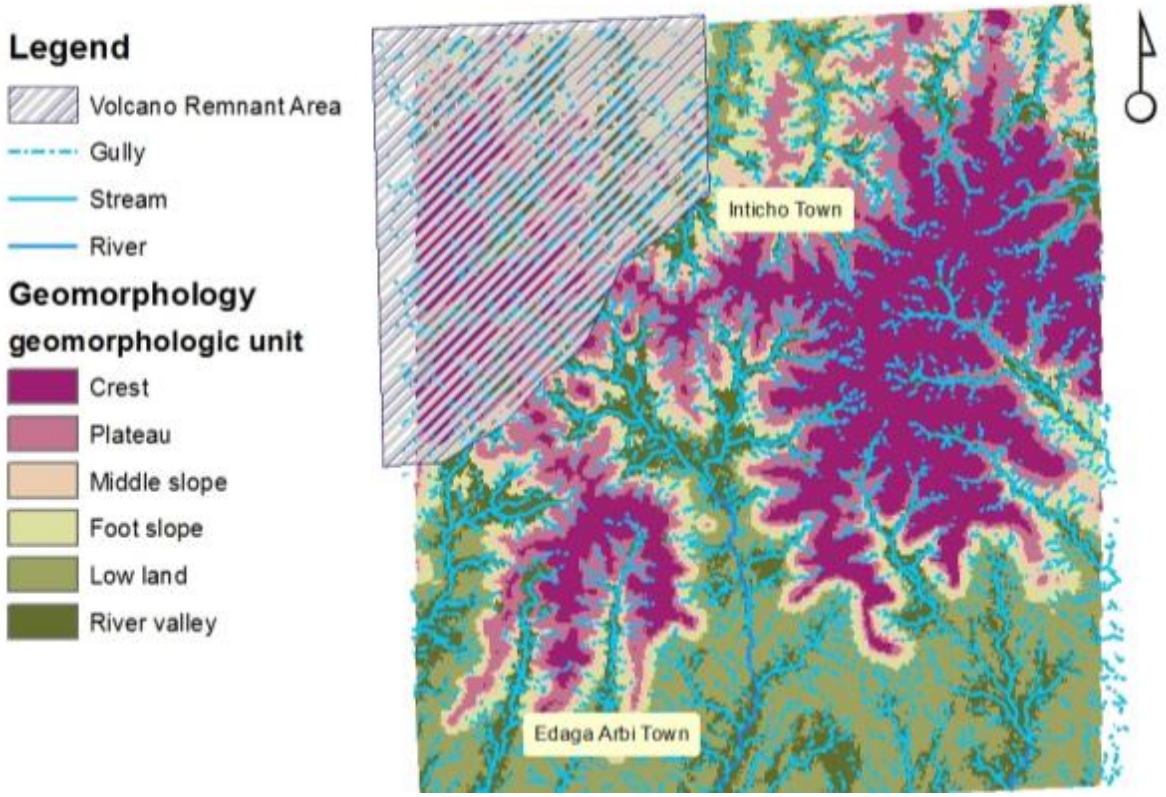

Figure 29: Representation of the geology (a) and geomorphology (b) based on the model from Table 3 with some corrections (a dip of 100 m in height over a distance of 50 km, corresponding to a slope of 0.2 % in south to north direction). In the south lies Edaga Arbi and in the north the town Inticho. The spatial distribution of the rocktypes seem very similar to the ones displayed in the map of Figure 3.

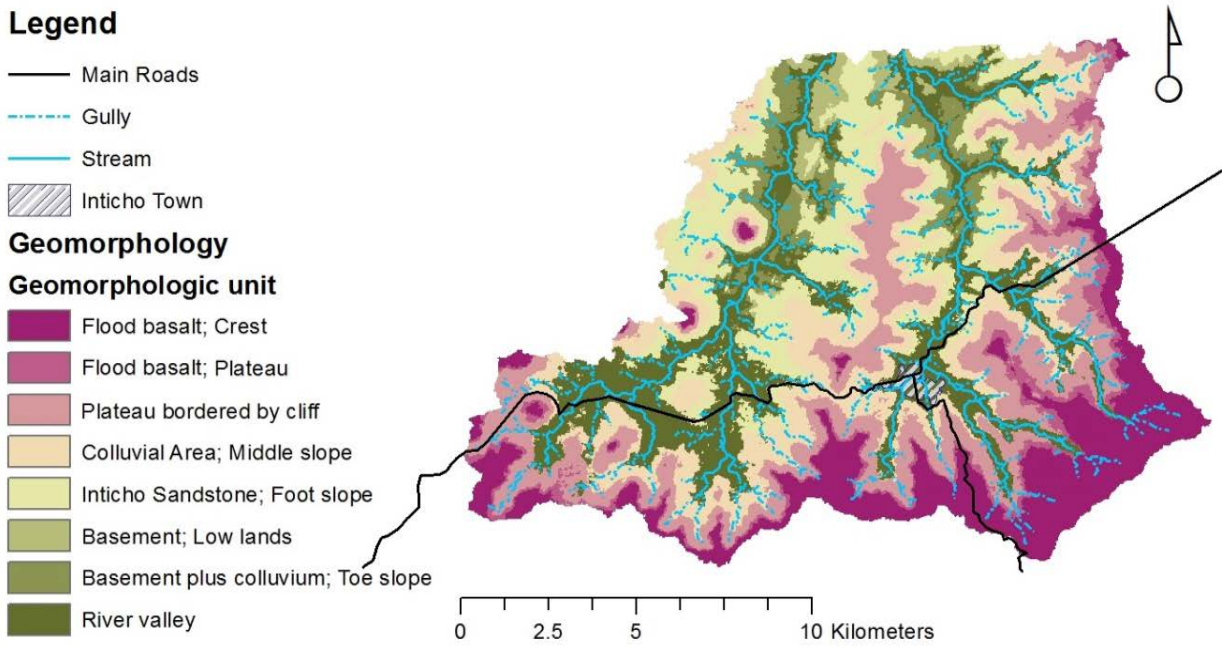

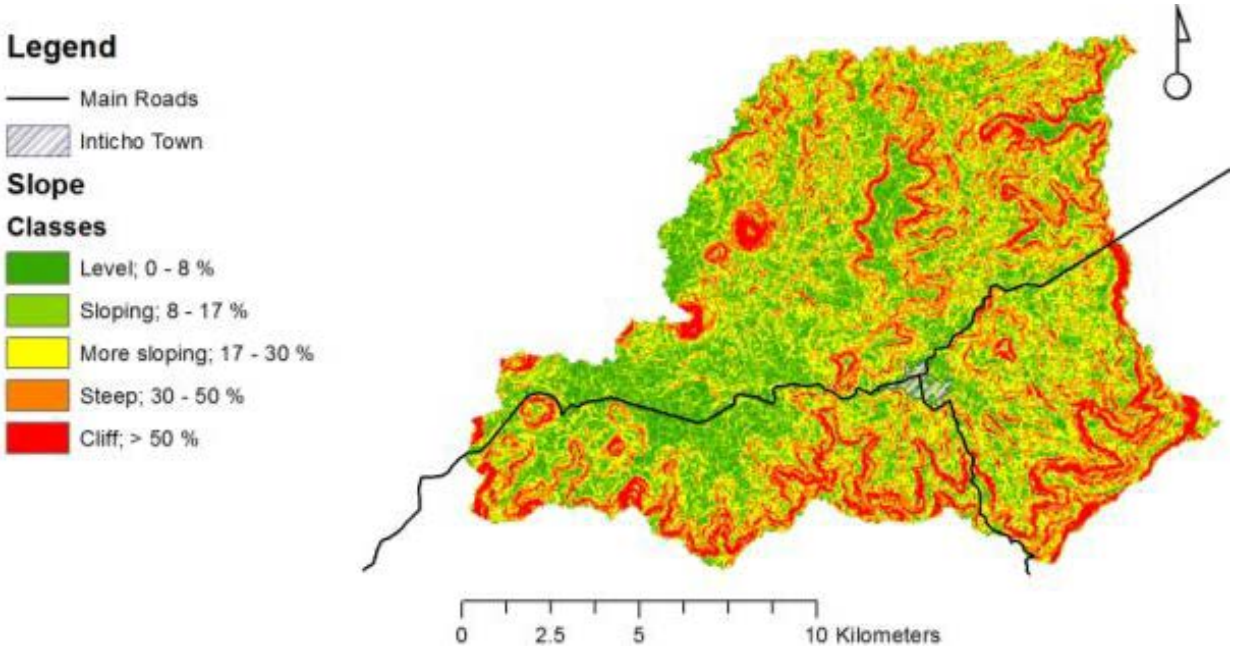

Figure 30: Geomorphology (a) and slope (b) in the Inticho study area. It is clear that the borders of geomorphological units are represented by steep slopes. One could relate this output with Figure 11.

Figure 30 illustrates that the geomorphological borders are, like in Edaga Arbi, the locations of steep slopes, although some steep slopes deviate from the classified border (especially more to the top of the map). Therefor can be concluded that the heights used in the classification in Edaga Arbi can also be applied in the Inticho region, but for future use, we should examine these locations to possibly fine-tune it. It should also be noted that the 'correction' used in the method (Section 3.3.2) misses this subtleness.

The modelling results for soil type in the Inticho basins and in close proximity of the town, can be seen in Figure 31.

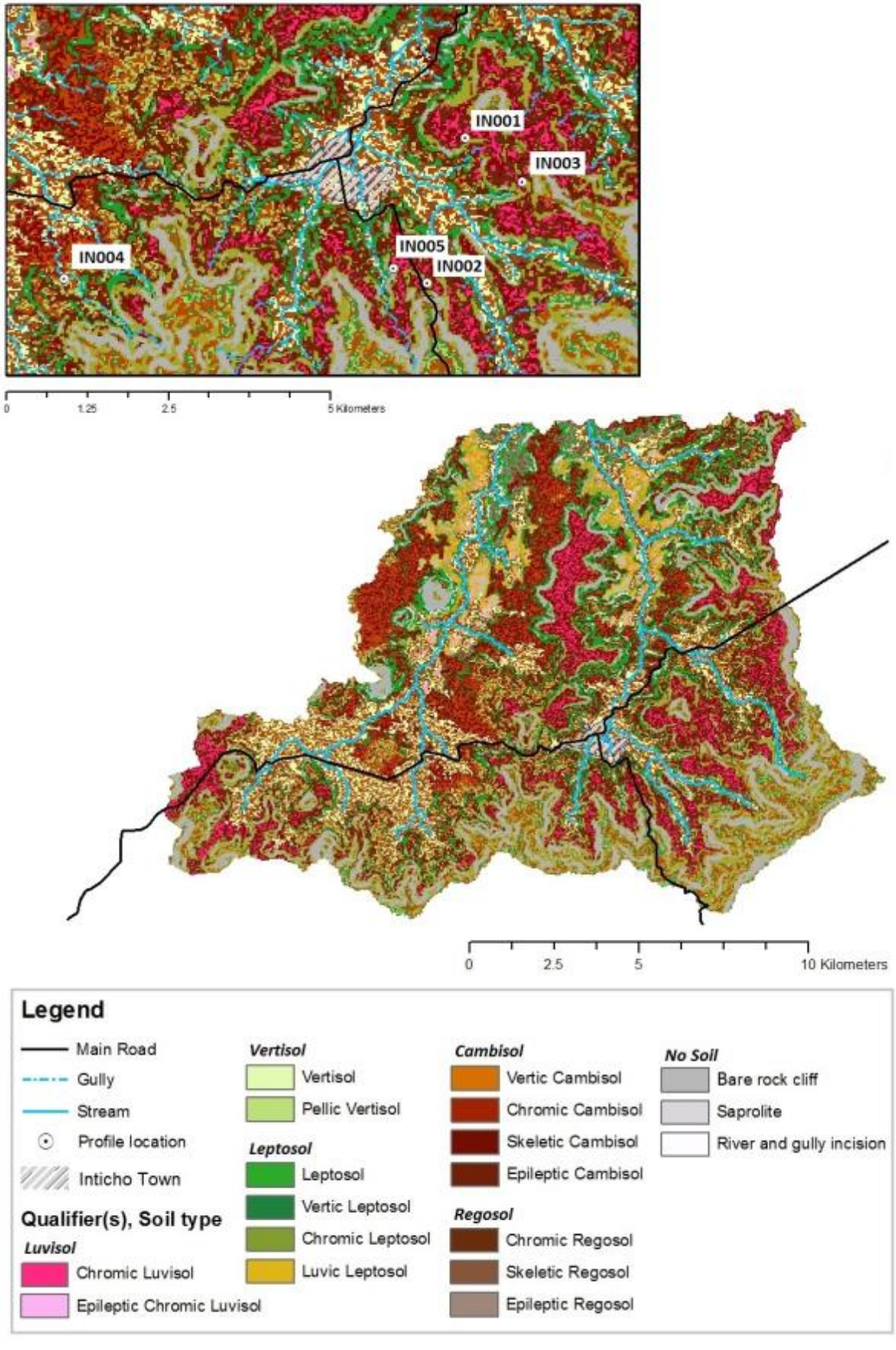

Figure 31: Soil type map of the 2 basins and a close-up of the surrounding of Inticho. The locations of 5 profile/sample points are indicated on the close-up map.

4.3.2 ACCURACY ASSESSMENT

5 observation/sample locations were visited in close proximity of Inticho town. The locations of those points are indicated in the inset window of Figure 31. The collected data is displayed in Table 16 and 17. Overall we see the same patterns in the landscape around Inticho as in the case of Edaga Arbi, but it must be noted that four of the five observations in Inticho happen to lay on the 'plateau' geomorphological unit. This is reflected in the smaller standard deviations (Table 16) compared to the values in Table 1 and 7. There are more observations needed, especially in the other geomorphologic units, to have a truly representable sample and be able to assess the true accuracy of this extrapolation attempt.

Table 16: Soil property values, mean and standard deviations of the sample points in the Inticho region.

Site-nr.	Surface Stoniness [%]	Munsell Value	Munsell Chroma	Munsell SOM [%]	pH	Nitrogen content [%]	SOM from N [%]	Clay Top [%]	Clay Sub [%]
IN001	80	3.0	3.0	3.0	7.0	0.13	2.8	40-60	>60
IN002	65	2.5	3.0	5.0	7.3	0.11	2.2	40-60	40-60
IN003	80	2.5	2.0	5.0	6.9	0.15	3.1	40-60	40-60
IN004	90	3.0	3.0	3.0	7.0	0.10	2.1	>60	>60
IN005	40	2.0	2.0	5.0	7.2	0.11	2.2	40-60	35-55
Mean	71	2.6	2.6	4.2	7.1	0.12	2.5	44-64	47-67
SD	17	0.37	0.49	0.98	0.15	0.018	0.37	9	12

Table 17: Profile descriptions of the profiles in the Inticho region. Abbreviations are according to the FAO guideline to soil description (reference); L = Loam, SiC = Silty clay, C = Clay, SCL = Sandy clay loam, HC = Heavy clay, SL = Sandy loam, CL = Clay loam, SC = Sandy clay, SiL = Silty loam; GR = granular, SB = sub-angular blocky, SG = single grained, MA = massive, WE = weak, MO = moderate, ST = strong, VF = very fine, FI = fine, ME = medium, CO = coarse, VC = very coarse.

Site-nr.	Horizon	Depth [cm]	Munsell Colour	Texture Class	Structure (type, grade, size)	Stone Content [%]	HCL
IN001	Ap	0-15	7.5YR	HC	GR ST ME	50	0
	Bt	15>25	7.5YR	HC	SB ST CO	50	
IN002	Ap	0-20	5YR	SiC	GR MO FI	40	0
	Ah	20-50	5YR	SiC	SB ST CO	40	
	Bt	50>80	5YR	HC	SB ST CO	40	
IN003	Ap	0-15	7.5YR	HC	SB WE ME	40	0
	Bt	15>90	7.5YR	HC	SB ST ME	20	
IN004	Ap	0-15	7.5YR	HC	GR ST FI	40	0
	Bt1	15-30	7.5YR	HC	SB ST CO	50	
	Bt2	30>60	7.5YR	HC	SB ST ME	50	
IN005	Ap	0-15	7.5YR	SiC	GR MO FI	10	0
	B1	15-30	7.5YR	SiC	SB ST ME	10	
	B2	30-45	7.5YR	SiC	SB ST ME	0	
	B3	45>90	5YR	SiC	SB ST ME	0	

Table 18: Soil profile (ground truth) vs. modelled soil type.

Site-nr.	Profile soil type	Model soil type
IN001	Skeletic clayic Cambisol	Chromic Luvisol
IN002	Skeletic Luvisol	Chromic Leptosol
IN003	Mollic Luvisol	Chromic Leptosol
IN004	Luvisol	Skeletic Regosol
IN005	Luvisol	Chromic Cambisol

Table 18 shows that, unfortunately, all of the observed soil types did not match the modelled ones. So one could state that the total accuracy of the model for this extrapolation site is 0%. A fist explanation could be that the geomorphologic units are positioned wrong. However, if the map (Figure 31) is studied in detail, it can be seen that the 'ground truth' soil type is in fact really close (30 to 100 m) to the profile location, but on a more flat location. The map is modelled with a 30 meter resolution. The soil profiles were on steep slope locations with terraces which were often only 5 meters in width. Although they are present everywhere in the study area, I did not consider the influence of these constructions on soil retention (they could be recent or ancient) and instead modelled these slopes to have more erosion resulting in Leptosols and Regosols instead of well-developed Luvisols.

5 GENERAL DISCUSSION

The validation of the extrapolation attempt shows that the locally designed decision tree model is unable to correctly predict the soil variability on a regional and detailed scale in the Northern Highlands of Ethiopia. However, it does sufficiently explain the spatial distribution of major soil types on a local scale. Soil texture and organic matter content were not sufficiently explained.

DSM techniques have been successfully applied with use of a limited amount of soil forming factors. This was the case in studies where soil variability is largely due to differences in topography, were the soil variability could be represented by elevation data and one terrain attribute only (.e.g. Florinsky et al. (2002)). This fact justifies the use of a limited amount of auxiliary information layers. In this case the availability was limited to only topography and vegetation. Nevertheless, the literature made clear that the soil development in the Northern Highlands of Ethiopia is not only correlated to topography. The most important explanatory variable is in fact parent material. Unfortunately there were no detailed geological maps, but locally this missing information could be drawn from the topography by defining geomorphological units under the assumption of horizontal layering. This geomorphology map became the most important branching sequence in the decision tree. On its own it already significantly explained the variation in soil colour, which is a strong reflection of parent material.

Although the prediction accuracy for soil type is sufficient, based on the threshold of 50%, it is slightly less than commonly found with DSM. For example, Taghizadeh-Mehrjardi et al. (2014) also applied a decision tree modelling approach to map major soil types, in Iran. Their attempt was successful, with an accuracy of 67%. They use a readily available geomorphological map in contrast to the topography based geomorphological interpretation (which is only representative under limiting assumptions) used here. Because the geomorphology is such a major factor, a correct geomorphology map is essential to inter- and extrapolation.

In case of the texture prediction, it was expected to behave similar to soil type (hence the same decision tree base), but the results showed a bigger variability within each group which was not correlated with any of the explanatory variables. The reason behind the variability could be the slope/mass movements that mix with and/or cover the original parent material.

Increasing the accuracy of delineating the geomorphological units, which are a major input to the model, would improve the accuracy of the predicted target variables. For this it is important to study the geology in more detail, but more specifically the (basaltic) mass movements. Delineating and identifying these from the DEM were very hard, with the current method. For this reason, Van de Wauw et al. (2008) took another approach. Their method is based on interpretation of ‘landform elements’ from differentiations in grey tone on aerial photographs (with a scale of 1:50 000), from which they could differentiate landslides. They choose to manually and visually delineate the geological features. Regardless of being labour-intensive and subjective, their model performs better than this one, suggesting that expert knowledge is indeed required in this particular study area.

The prediction of soil organic matter, based on environmental properties only, is usually more difficult and similar prediction accuracies like this one are also encountered in other studies (e.g. Stoorvogel et al. (2009) and Mora-Vallejo et al. (2008)). A possible reason for the low prediction accuracy, is that the SOM content is strongly influenced by management practices. This is a soil

forming factor that is not included in this research, because it requires a far more intensive sampling strategy. The only way to try to implement it was to use the available NDVI data. In the study of Vågen et al. (2013), the use of Landsat reflectance data was very successful in predicting SOC contents. Regrettably, the results of this study showed that the vegetation density only explains a very small fraction of the observed variability. From farm surveys it is known that farmers across the study area use different soil management that can have different effect on soil properties, particularly SOM. This is especially true for parts that are terraced, because of soil redistribution processes.

Predictive soil mapping has been most successful at the local scale, because many of the soil-forming factors can be held constant (Scull et al. 2003). This is one of the important reasons for the successful prediction on the local scale, followed by an unsuccessful extrapolation. Climate was also indicated by literature to be of importance to soil development. This factor was of insignificant importance on the local scale, but regionally differences can be noticed. Rainfall patterns and temperature differ between the four towns, which is reflected in growing seasons that are shifted in relation to each other.

After the extrapolation result was studied in detail, it became clear that the modelled soil-landscape relations were actually more or less right, but the resolution of the prediction could not manage the higher soil variability due to the existence of narrow terraces (5 – 10 m) on steep slopes. The choice of the current resolution was based on the research of Cavazzi et al. (2013), who stated that morphologically varied areas, like this one, with characteristic features or abrupt changes in topography reflected in steep slopes, prefer fine resolutions (30m) for a better prediction accuracy. But my findings suggest that an even finer resolution might be required.

For all field observations and measurements counts that the values were not calibrated with laboratory results. This influences both the model development and the validation, because it causes uncertainty of the measurement error. If the measurement error is large, this reflects on the prediction being inaccurate. Overall it would have been better to have laboratory results, although it proved to be problematic in underdeveloped countries such as Ethiopia.

So, the low prediction accuracies can be dedicated to a large uncertainty and insignificant differences for most variables in the model through improper delineation of geomorphologic units, possible field measurement error and missing soil forming factors. However, there is a simple solution that could bring direct improvements to the model. Namely proper calibration of the initial estimates (the outputs at the end of each branch in the decision tree). As said before, this requires additional data in the form of a ‘calibration dataset’ or additional validation data to be able to perform a cross-validation. The sample size was deliberately kept very small, in order to decrease research costs; 14 observation and sample points make up the transect dataset, 32 the validation dataset and only 5 were available to validate the extrapolation. This number has shown to be insufficient, when this kind of detail is required.

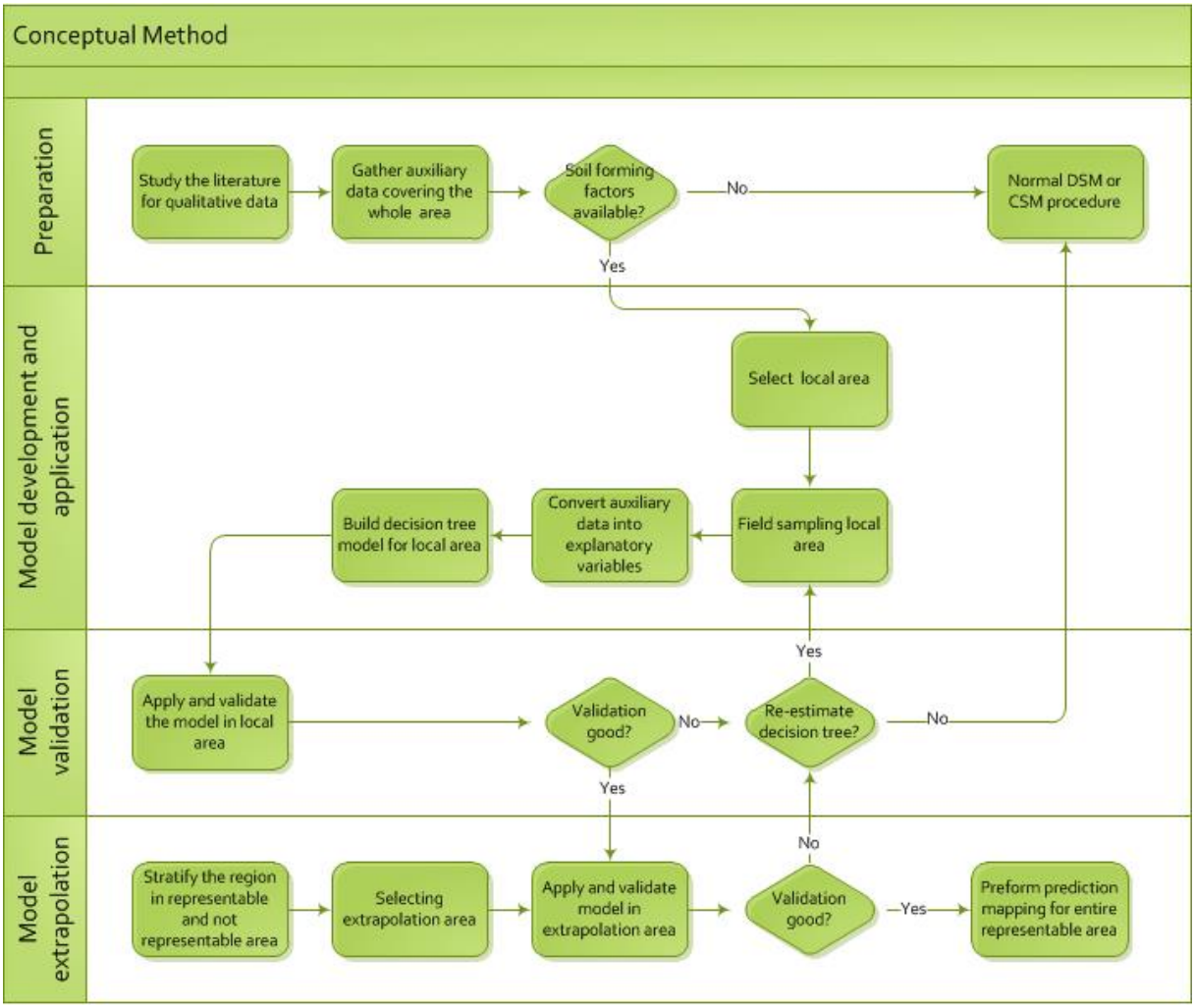

Figure 32: The new conceptual method in cases of limited data availability.

One of the limitations of decision tree modelling is the discrete predictions from each terminal node, what results in the lack of smoothness of the prediction surface. Especially a continuous soil property like texture and SOM can be misrepresented. An improvement to the structure of the tree is to build multivariate linear models in each node (leaf). To further improve the prediction, we could apply fuzzy memberships to allow a smoother transition from one class to another (Scull et al. 2003, McBratney et al. 2003, Wang et al. 2012). But this would also require more sample points.

This study is still constrained by the limited number of samples and auxiliary information. As Mora-Vallejo et al. (2008) point out, the selection of the explanatory variables remains rather arbitrary. Even in an environment with relatively little data available, an almost infinite number of explanatory variables can be defined that characterize the key soil forming processes. Insight in the agro-ecological conditions in the region may help to select the most important ones. Therefore, it should be pointed out that some alteration to the conceptual method (Figure 1) is in place. Figure 32 shows the updated flowchart of the approach. An additional step (preparation) indicates the importance to consider that you have the right soil forming factors represented by the available auxiliary information to continue to model development.

New sampling techniques through proximal sensing with spectrometry allow for a rapid assessment and could allow for more sample points. It is unfortunate that the method of Stoorvogel et al. (2013),

for field measurement of soil texture could not be examined further. It could have given a detailed insight in the texture variability at a relatively low cost.

In further research, another mechanistic approach could help delineate the mass-movements and landslides with use of the limited available auxiliary information. For example the dynamic landscape evolution model LAPSUS (Schoorl, Veldkamp and Bouma 2002) could open possibilities into studying the dynamics of these mass movements that are so hard to classify. Claessens, Schoorl and Veldkamp (2007) were able to model the location of landslides in a large catchment.

6 CONCLUSION

In contrast to many other soil mapping surveys, in which an ordinary DSM or CSM strategy is used, this is a study in which a more qualitative approach to DSM is used. This study is different as it lacked an extensive training dataset to use to estimate the relationships between soil properties and auxiliary information. Instead qualitative information in the form of soil catenas and soil classification surveys were used to develop decision tree models for soil type, texture class and organic matter content. This approach is cost and time efficient in situations of poor accessibility and limited quantitative data availability.

Although the limited amount of samples and auxiliary information clearly constrained the prediction, the decision tree model could successfully map major soil type at a high resolution of a local area in the poorly accessible and heterogenic landscape in the Northern Highlands of Ethiopia. To understand the diversity and the distribution of the soils, the most important parameter is to identify the parent material. In addition, identifying and delineating mass movement bodies is advised. However, there was no detailed auxiliary information available for geology. In return, the two important soil forming factors implemented in the model were geomorphology and slope (both derived from the DEM). Increasing the accuracy of the geomorphology interpretation would increase the prediction accuracy of the model. The remaining variability could be explained by a third important soil forming factor, namely soil management. This factor was not implemented in the model. For a successful extrapolation of the model, additional information on geology and climate are needed or a more conventional method should be applied.

The conceptual method has potential to be implemented globally and cost-effectively in situations where detail is required under limiting circumstances, but under the condition that the right auxiliary information is available. It should be noted that in large areas soil forming processes are rarely uniform and considerations at watershed level should be taken.

ACKNOWLEDGEMENTS

I want to thank Jetse Stoorvogel and Richard Kraaijvanger for their valuable time and guidance to enhance the quality of this work. Furthermore I am very thankful to Richard Kraaijvanger and his family for welcoming me and Henrieke into their home in Ethiopia, their kindness and support will never be forgotten. In turn, I also want to acknowledge Henrieke for the wonderful time we shared together.

I would like to express my deepest respect and gratitude towards Marthijn Sonneveld, who has inspired me in many things, of which one is this research. His death is still very painful. I will miss his advice and calm teachings.

I also like to thank my boyfriend Stefan for all his belief and support, when I was away from home for three months and his patience and tolerance when I was working in Wageningen, and came home late with my mind still occupied with thesis stuff. I also really appreciate all those lunches he made for me!

REFERENCES

Araya, A., S. D. Keesstra & L. Stroosnijder (2010) A new agro-climatic classification for crop suitability zoning in northern semi-arid Ethiopia. *Agricultural and Forest Meteorology,* 150**,** 1057-1064.

Berakhi, O., L. Brancaccio, G. Calderoni, M. Coltorti, F. Dramis & M. M. Umer (1998) The Mai Maikden sedimentary sequence: a reference point for the environmental evolution of the Highlands of northern Ethiopia. *Geomorphology,* 23**,** 127-138.

BoANR-LUPRD. 2000. Indicative Master Land Use Plan, Soil Survey Section. Mekelle, Ethiopia. .

Boon, J. 2012. Edaga-Arbi tillites below Adigrat sandstone. ed. 20.jpg. KU Leuven.

Cambule, A. H., D. G. Rossiter & J. J. Stoorvogel (2012) A methodology for digital soil mapping in poorly-accessible areas. *Geoderma,* 192**,** 341-353.

Cavazzi, S., R. Corstanje, T. Mayr, J. Hannam & R. Fealy (2013) Are fine resolution digital elevation models always the best choice in digital soil mapping? *Geoderma,* 195-196**,** 111-121.

Claessens, L., J. M. Schoorl & A. Veldkamp (2007) Modelling the location of shallow landslides and their effects on landscape dynamics in large watersheds: An application for Northern New Zealand. *Geomorphology,* 87**,** 16-27.

De Mûelenaere, S., A. Frankl, M. Haile, J. Poesen, J. Deckers, N. Munro, S. Veraverbeke & J. Nyssen (2012) Historical landscape photographs for calibration of landsat land use/cover in the northern ethiopian highlands. *Land Degradation and Development*.

Eijkelkamp. 2004. Operating Instructions for the Nitrachek reflectometer. http://pkd.eijkelkamp.com/Portals/2/Eijkelkamp/Files/Manuals/M1-1840e%20Nitracheck%20reflectometer.pdf.

FAO. 2006. Guidelines for soil description. Rome, Italy: Food and agriculture organisation of the united nations.

Florinsky, I. V., R. G. Eilers, G. R. Manning & L. G. Fuller (2002) Prediction of soil properties by digital terrain modelling. *Environmental Modelling and Software,* 17**,** 295-311.

GADM. 2012. GADM database of Global Adminitrative Areas.

Girmay, D. 2006. Geological characteristics and economic evaluation of oil shale deposits in Tigray, Ethiopia. In *26th Oil shale symposium*. Colorado school of mines: Tigray Region Bureau of Water Resource, Mines and Energy, Ethiopia and Mekelle University, Department of Applied Geology, Mekelle, Ethiopia.

Girmay, G. & B. R. Singh (2012) Changes in soil organic carbon stocks and soil quality: Land-use system effects in northern Ethiopia. *Acta Agriculturae Scandinavica Section B: Soil and Plant Science,* 62**,** 519-530.

Girmay, G., B. R. Singh. & D. Øystein (2010) Land-use changes and their impacts on soil degradation and surface runoff of two catchments of Northern Ethiopia. *Acta Agriculturae Scandinavica Section B: Soil and Plant Science,* 60**,** 211-226.

GoogleEarth. 2013, December 13. Satellite Image: Mymisham Ridge, Edaga Arbi, Tigray, Ethiopia 2013. In *Google Earth V7.1.2.2041*, Lat 14.048977 Lon 39.054494 Eye altitude 12.74 km. Digital Globe 2014.

Hagos, M., C. Koeberl, K. Kabeto & F. Koller (2010) Geochemical characteristics of the alkaline basalts and the phonolite-trachite plugs of the Axum area, northern Ethiopia. . *Australian Journal of Earth Sciences* 103**,** 153-170.

Hengl, T., G. B. M. Heuvelink & A. Stein (2004) A generic framework for spatial prediction of soil variables based on regression-kriging. *Geoderma,* 120**,** 75-93.

Houten, J. V. 2002. A canyon west of Adigrat in northern Tigray, Ethiopia*.,* ed. Canyon16.jpg. Wikipedia.

Kempen, B., D. J. Brus, J. J. Stoorvogel, G. B. M. Heuvelink & F. De Vries (2012) Efficiency comparison of conventional and digital soil mapping for updating soil maps. *Soil Science Society of America Journal,* 76**,** 2097-2115.

Kraaijvanger, R. 2013. PE&RC-08060-Working document I: Phase 1 (2008-2009).

Kraaijvanger, R., M. P. W. Sonneveld, C. M. A. Almekinders & A. Veldkamp. 2013. Comparing approaches for identification of productivity constraints and oppartunities in marginal farming systems in central Tigray, Ethiopia.

Kumpulainen, R. A., A. Uchman, B. Woldehaimanot, T. Kreuser & S. Ghirmay (2006) Trace fossil evidence from the Adigrat Sandstone for an Ordovician glaciation in Eritrea, NE Africa. *Journal of African Earth Sciences,* 45**,** 408-420.

McBratney, A. B., M. L. M. Santos & B. Minasny (2003) On digital soil mapping. *Geoderma,* 117**,** 3-52.

Merla, G., Abbate, E., Azzaroli, A., Bruni, P., Canuti, P., Fazzuoli, M., Sagri, M., Tacconi, P. . 1973. A Geological Map of Ethiopia and Somalia (1973) 1:2.000.000 and Comment. . ed. I. University of Florence.

METI & NASA. 2011. Advanced Spaceborne Thermal Emission and Reflection Radiometer (ASTER) Global Digital Elevation Model Version 2 (GDEM V2). Extent (top, left, right, bottom): 14.5001388889; 38.4998611111; 39.5001388889; 13.4998611111. Spatial reference: GCS_WGS_1984 Spatial resolution: 27 m. The Ministry of Economy, Trade, and Industry (METI) of Japan and the United States National Aeronautics and Space Administration (NASA).

Mohr, P. 1663. The Geology of Ethiopia. . University College of Addis Ababa Press, p.270.

Mora-Vallejo, A., L. Claessens, J. Stoorvogel & G. B. M. Heuvelink (2008) Small scale digital soil mapping in Southeastern Kenya. *CATENA,* 76**,** 44-53.

Nyssen, J., J. Naudts, K. De Geyndt, M. Haile, J. Poesen, J. Moeyersons & J. Deckers (2008) Soils and land use in the Tigray Highlands (Northern Ethiopia). *Land Degradation and Development,* 19**,** 257-274.

Nyssen, J., J. Poesen, J. Moeyersons, J. Deckers, M. Haile & A. Lang (2004) Human impact on the environment in the Ethiopian and Eritrean highlands - A state of the art. *Earth-Science Reviews,* 64**,** 273-320.

Nyssen, J., H. Vandenreyken, J. Poesen, J. Moeyersons, J. Deckers, M. Haile, C. Salles & G. Govers (2005) Rainfall erosivity and variability in the Northern Ethiopian Highlands. *Journal of Hydrology,* 311**,** 172-187.

Rabia, A. H., R. R. Afifi, A. M. Gelaw, S. Bianchi & H. *e. a.* Figueredo (2013) Soil mapping and classification: a case study in the Tigray Region, Ethiopia. *Journal of Agriculture and Environment for International Development - JAEID,* 107**,** 73-99.

Schoorl, J. M., A. Veldkamp & J. Bouma (2002) Modeling water and soil redistribution in a dynamic landscape context. *Soil Science Society of America Journal,* 66**,** 1610-1619.

Scull, P., J. Franklin, O. A. Chadwick & D. McArthur (2003) Predictive soil mapping: a review. *Progress in Physical Geography,* 27**,** 171-197.

Stoorvogel, J. J., C. Hendriks & L. Claessens. 2013. Field procedure for measuring the soil texture. Wageningen: Wageningen University.

Stoorvogel, J. J., B. Kempen, G. B. M. Heuvelink & S. de Bruin (2009) Implementation and evaluation of existing knowledge for digital soil mapping in Senegal. *Geoderma,* 149**,** 161-170.

Taghizadeh-Mehrjardi, R., F. Sarmadian, B. Minasny, J. Triantafilis & M. Omid (2014) Digital Mapping of Soil Classes Using Decision Tree and Auxiliary Data in the Ardakan Region, Iran. *Arid Land Research and Management,* 28**,** 147-168.

Tesfamichael, G. D. S., F.; Miruts, H.; Solomon, G.; Kassa, A.; Kurkura, K.; Abdulwassie, H.; Bauer, H.; Nyssen, J.; Moeyersons, J.; Deckers, J.; Mitiku, H.; Nurhussen, T. 2010. Large-Scale Geological mapping of the Geba basin, northern Ethiopia. In *Tigray Livelihood Paper No 9*, 46 pp. Mekelle, Ethiopia: VLIR – Mekelle University IUC Program.

USAID. 2007. Trends in Demographic and Reproductive Health Indicators in Ethiopia. In *ETHIOPIA TREND REPORT*. Calverton, Maryland, USA: Macro International Inc.

USDA. 2013. Three major rainfall regimes for Ethiopia. In *Production Estimates and Crop Assesment Division (PECAD)*. USDA.

USGS. 2005. Landsat 7 ETM+ Multispectral image. Extent (top, left, right, bottom): 14.5001388889; 38.4998611111; 39.5001388889; 13.4998611111. Spatial reference: GCS_WGS_1984 Spatial resolution: 30 m. United States Geological Survey, Earth Resources Observation and Science (EROS) Center

Vågen, T.-G., L. A. Winowiecki, A. Abegaz & K. M. Hadgu (2013) Landsat-based approaches for mapping of land degradation prevalence and soil functional properties in Ethiopia. *Remote Sensing of Environment,* 134**,** 266-275.

Van de Wauw, J., G. Baert, J. Moeyersons, J. Nyssen, K. De Geyndt, N. Taha, A. Zenebe, J. Poesen & J. Deckers (2008) Soil–landscape relationships in the basalt-dominated highlands of Tigray, Ethiopia (Environmental change, geomorphic processes and land degradation in tropical highlands). *CATENA,* 75**,** 117-127.

Vancampenhout, K., J. Nyssen, D. Gebremichael, J. Deckers, J. Poesen, M. Haile & J. Moeyersons (2006) Stone bunds for soil conservation in the northern Ethiopian highlands: Impacts on soil fertility and crop yield. *Soil and Tillage Research,* 90**,** 1-15.

Wang, D.-C., G.-L. Zhang, X.-Z. Pan, Y.-G. Zhao, M.-S. Zhao & G.-F. Wang (2012) Mapping Soil Texture of a Plain Area Using Fuzzy-c-Means Clustering Method Based on Land Surface Diurnal Temperature Difference. *Pedosphere,* 22**,** 394-403.

Yami, M., W. Mekuria & M. Hauser (2013) The effectiveness of village bylaws in sustainable management of community-managed exclosures in Northern Ethiopia. *Sustainability Science,* 8**,** 73-86.